AEDC-TR-69-86

C#1

cy 1

REDUCTION OF WALL INTERFERENCE EFFECTS IN THE AEDC-PWT 1-FT TRANSONIC TUNNEL WITH VARIABLE PERFORATED WALLS

J. L. Jacocks

ARO, Inc.

May 1969

PROPULSION WIND TUNNEL FACILITY
ARNOLD ENGINEERING DEVELOPMENT CENTER
AIR FORCE SYSTEMS COMMAND
ARNOLD AIR FORCE STATION, TENNESSEE

NOTICES

When U. S. Government drawings specifications, or other data are used for any purpose other than a definitely related Government procurement operation, the Government thereby incurs no responsibility nor any obligation whatsoever, and the fact that the Government may have formulated, furnished, or in any way supplied the said drawings, specifications, or other data, is not to be regarded by implication or otherwise, or in any manner licensing the holder or any other person or corporation, or conveying any rights or permission to manufacture, use, or sell any patented invention that may in any way be related thereto.

Qualified users may obtain copies of this report from the Defense Documentation Center.

References to named commercial products in this report are not to be considered in any sense as an endorsement of the product by the United States Air Force or the Government.

REDUCTION OF WALL INTERFERENCE EFFECTS IN THE AEDC-PWT 1-FT TRANSONIC TUNNEL WITH VARIABLE PERFORATED WALLS

J. L. Jacocks
ARO, Inc.

FOREWORD

The work reported herein was sponsored by Headquarters, Arnold Engineering Development Center (AEDC), Air Force Systems Command (AFSC), Arnold Air Force Station, Tennessee, under Program Element 65401F/06RB.

The results of research presented were obtained by ARO, Inc. (a subsidiary of Sverdrup & Parcel and Associates, Inc.) contract operator of AEDC, AFSC, under Contract F40600-69-C-0001. The research was conducted from October 8 to October 24, 1968, under ARO Project No. PA2917, and the manuscript was submitted for publication on March 12, 1969.

Information in this report is embargoed under the Department of State International Traffic in Arms Regulations. This report may be released to foreign governments by departments or agencies of the U. S. Government subject to approval of the Arnold Engineering Development Center (AETS), or higher authority within the Department of the Air Force. Private individuals or firms require a Department of State export license.

This technical report has been reviewed and is approved.

Richard W. Bradley
Lt Colonel, USAF
AF Representative, PWT
Directorate of Test

Roy R. Croy, Jr.
Colonel, USAF
Director of Test

ABSTRACT

An experimental investigation was conducted in the 1-Ft Transonic Tunnel to assess the transonic wave cancellation performance of six variable porosity, test section wall designs. The wall interference effects were detected utilizing a 20-deg cone-cylinder static pressure model of 1-percent blockage. The variable wall porosity designs incorporated a sliding cutoff plate with hole geometry identical to a fixed airside plate. Upstream movement of the sliding plates for decreasing porosity provided a test section boundary which successfully eliminated wave reflection wall interference throughout most of the transonic range.

CONTENTS

APPENDIX

Illustrations

NOMENCLATURE

d	Model diameter, in.
M_N	Nominal Mach number
p	Static pressure, psfa
p_t	Stagnation pressure, psfa
x	Model station, in.
θ_w	Test section wall angle, deg (positive diverged)
τ	Wall porosity, percent

SECTION I
INTRODUCTION

The problem of wall interference effects in transonic wind tunnels has received much study at AEDC as well as at other facilities. Operational test section wall design concepts have included slots, perpendicular holes or perforations, inclined holes, and combinations of these. Reference 1 demonstrated that the 60-deg inclined hole, 6-percent open wall design virtually eliminated both compression and expansion wave reflections at Mach number 1.2. It was also shown in Ref. 1 that similar reductions in wall interference could be obtained at other Mach numbers if the wall porosity was changed as a function of Mach number.

The desirability of providing variable wall porosity has been recognized in the design of several new transonic wind tunnels. The 14 x 14-inch Trisonic Wind Tunnel at the Marshall Space Flight Center incorporates a fixed airside test section wall and a sliding cutoff plate with downstream motion to provide a porosity range from 0 to 5.4 percent with 60-deg inclined holes. Pressure distribution data (Ref. 2) on a 0.9-percent blockage 20-deg cone-cylinder model in this tunnel are practically interference free throughout the Mach range from 0.90 to 1.25.

A similar wall design (60-deg inclined holes with a porosity range from 0 to 10 percent) was applied to the new 4-ft transonic tunnel (Aerodynamic Wind Tunnel, Transonic (4T)) at AEDC. Initial calibration of Tunnel 4T, Ref. 3, revealed that for supersonic Mach numbers a severe overexpansion occurred at the end of the conventional tapered porosity region. This overexpansion was followed by a strong compression and subsequent virtually undamped reflection of the disturbances throughout the test section. Reduction of the maximum wall porosity from 10 to 6.7 percent by plugging every third hole did not significantly affect the flow. The overexpansion was finally eliminated by a trial and error tailoring of the tapered porosity region. Subsequent tests with a 1-percent blockage, 20-deg cone-cylinder model showed that the walls could not cancel both compression and expansion waves at a given porosity, although some improvement relative to a fixed porosity wall was evident.

Since two tunnels with virtually identical design had yielded such widely different results, an experimental study (Ref. 4) was made of the crossflow characteristics of the variable porosity wall design. The major conclusion of the study was that improved wall characteristics could be obtained by moving the cutoff plate in any direction other than

downstream (Refs. 2 and 3 both indicate downstream movement), but the tests were not sufficiently definitive to allow a more positive recommendation.

In an effort to obtain definitive data, the present tests were conducted in the 1-ft transonic tunnel (Aerodynamic Wind Tunnel, Tunnel (1T)) utilizing a 1-percent blockage, 20-deg cone-cylinder model installed in a new variable porosity test section. The test section wall design was scaled from Tunnel 4T with additional provisions for moving the cutoff plate in any direction. The ability of the walls to alleviate wave reflection interference is inferred from static pressure distributions on the cone-cylinder model. Data are presented for six discrete cutoff plate movement concepts at various wall porosity settings through the Mach range from 0.95 to 1.20. Scaling effects upon the wall performance are shown by comparisons with data obtained in Tunnel 4T. Mach number calibration data for the optimum wall configuration in Tunnel 1T are presented in Ref. 5.

SECTION II
APPARATUS

2.1 TUNNEL 1T

The 1-ft transonic tunnel is a continuous-flow, nonreturn wind tunnel equipped with a two-dimensional, flexible nozzle and an auxiliary plenum evacuation system. The Mach number range is normally from 0.2 to 1.5 utilizing variable nozzle contours above $M_N = 1.1$. For the present study, the nozzle was fixed on the sonic contour. The test section is 37.5 in. long and 12 by 12 in. in cross section. The top and bottom walls are supported by flexures at the nozzle exit and screw actuators at the downstream end to provide for variation in wall angle.

The general arrangement of the tunnel and its associated equipment is shown in Fig. 1 of the Appendix. A detailed description of the tunnel is given in Ref. 6.

2.2 TEST SECTION WALLS

The airside test section wall geometry is shown in Fig. 2. The maximum wall porosity (10 percent) is defined to be the area of the holes, based upon the diameter, divided by the total wall area. The Tunnel 4T walls are 3/8 in. thick, but the Tunnel 1T walls are 1/8 in. thick so that

exact scaling was not maintained. However, the hole pattern and ratio of hole diameter to plate thickness are the same in both tunnels. The hole pattern shown in Fig. 2 is applicable to the bottom and north walls, but the top and south wall hole patterns are mirror images of the figure. This reversal of the pattern also exists in Tunnel 4T.

The variable porosity feature is obtained by using a sliding cutoff plate with identical hole geometry and thickness as the airside plate. The various cutoff plate configurations are sketched in Fig. 3. For convenience, the geometries are designated by the letters A through F. Wall configuration A represents the original Tunnel 4T design with the cutoff plate sliding downstream for decreasing porosity. Walls B, C, and D are transverse, upstream, and 30-deg skewed-upstream movements of the cutoff plate, respectively. Walls E and F were obtained by interchanging the cutoff plates between the top and bottom and the north and south walls.

Each plate was individually fabricated from sheet aluminum utilizing numerical control machining which provided acceptable hole alignment.

A photograph of the back of the south wall is presented in Fig. 4. Inside micrometers were used at the jack-screw fixtures shown in the picture to position the cutoff plates. The positioning error was less than ±0.003 in. relative to the full-open setting. However, the full-open setting was somewhat arbitrary, particularly for walls E and F. The holes were visually aligned for the full-open position, and this setting error is estimated to be ±0.010 in.

The functional relationship between wall porosity and cutoff plate position is shown in Fig. 5. The wall porosity is defined as the open area at the cutoff section projected along the airside hole axis divided by the hole area and multiplied by the maximum wall porosity (10 percent). For all configurations, the projected open area is formed by segments of two circles.

2.3 CONE-CYLINDER MODEL

A sketch of the 20-deg cone-cylinder model showing the pressure orifice locations is given in Fig. 6. Through fabrication error, the cone angle is 18 minutes shallow. An installation sketch is given in Fig. 7, and a photograph of the installation is presented as Fig. 8.

The model orifices were relatively small, 0.023 in., and it was difficult to remove the burrs resulting from final machining. The data

from a few of the orifices are not presented because of consistently high or low pressure measurements which were attributed to these burrs.

2.4 INSTRUMENTATION

Basic tunnel instrumentation consisted of a copper-constantan thermocouple grid for stagnation temperature, a servodriven mercury manometer for plenum pressure, and a precision pressure gage for stagnation pressure. The model pressures were photographically recorded from a multitube mercury manometer board referenced to atmospheric pressure.

SECTION III
PROCEDURE

3.1 TEST CONDITIONS

Stagnation pressure control is not available in Tunnel 1T. For the present study, the stagnation pressure was 2750 ± 50 psf. Stagnation temperature was maintained as required to prevent visible condensation, the range being from 140 to 170°F. Model pressure distributions were obtained at nominal Mach numbers of 0.95, 1.00, 1.05, 1.10, 1.15, and 1.20 with the sonic nozzle contour.

Tunnel calibrations have not been conducted with all wall configurations of the present study. The Mach number was set by visually comparing the model afterbody pressures with an overlay on the manometer board. These Mach number settings were not too precise because of wall interference effects and the day-to-day variations in tunnel stagnation pressure.

3.2 DATA REDUCTION AND PRECISION

The photographically recorded manometer data were reduced to pressure ratios, p/p_t, using semiautomatic film reading equipment in conjunction with an offline computer program. All data were computer-plotted and traced for this presentation.

Based on a confidence level of 95 percent, estimates of the random errors in the data are:

ΔM_N	±0.03
$\Delta p/p_t$	±0.003
$\Delta \theta_w$	±0.1
$\Delta \tau$	±0.15

SECTION IV
RESULTS AND DISCUSSION

4.1 CENTERLINE MACH NUMBER DISTRIBUTIONS

Representative Mach number distributions obtained in Tunnels 4T and 1T with wall configuration A (Refs. 3 and 5) are compared in Fig. 9. The axial tunnel stations are normalized by the tunnel heights with station zero defined to be at the downstream end of the tapered porosity regions. The differences among the data from the two tunnels are apparently attributable to Reynolds number and hole-size effects since other parameters are properly scaled. However, the significant point is that the data correspond qualitatively, this being particularly evident in Fig. 9b with 5-percent porosity. The Mach number gradients within the tapered porosity regions show that a given wall porosity is effectively more open in Tunnel 1T than in Tunnel 4T.

4.2 INFLUENCE OF WALL GEOMETRY AND POROSITY

Pressure distributions on the 20-deg cone-cylinder model can be better understood with the aid of Fig. 10. Initial reflections of the model-induced disturbances impinge upon the model at the approximate stations shown. If the wall possesses the desired wave cancellation characteristics, the model pressures will show no perturbations at these specific body stations.

The model pressure distributions are compared in Figs. 11 through 18 with interference-free curves (designated I. F.) that are based upon theory and upon empirical results from Refs. 1 and 7. The error in cone angle results in a corresponding error in I. F. pressure ratio less than 0.002, which was considered insignificant.

Model pressure distributions obtained with wall A are presented in Fig. 11. Also shown for comparison are previously unpublished results from Tunnel 4T where available. Except for slight differences caused by Mach number variations, the data from the two tunnels are in agreement.

The near perfect agreement evident in Fig. 11b, in spite of the large Mach number variations shown in Fig. 9b, is partially a result of chance location of the models in the test sections. For Tunnel 4T the model nose was placed at normalized station 0.75, whereas for Tunnel 1T the nose was at station 0.58; the difference between these stations corresponds with the axial Mach number shift between the two tunnels.

The general accordance of both the model pressures and the Mach number distributions from Tunnels 1T and 4T indicates that conclusions derived from the present results will be applicable to most transonic wind tunnels and to Tunnel 4T in particular.

The interference effects evident in Fig. 11 are primarily compression waves impinging on the model that originate from the downstream portion of the shoulder-induced expansion field. That wall A does not possess the proper characteristics is conclusively shown at $M_N = 1.05$, $\tau = 2$. The bow wave is reflected onto the model nose as a compression, and the expansion field also reflects as a compression. This result implies that the 2-percent wall porosity setting is effectively too closed for outflow from the test section, yet too open for inflow. The 4-percent porosity setting (Fig. 11b) provides reasonable compression wave cancellation at $M_N = 1.20$, but it is too open to cancel the expansion field.

Model pressure distributions with transverse wall movement (wall B) are presented in Fig. 12 for $\tau = 1$, 2, 3, and 6. The performance of this wall configuration is acceptable at $M_N = 1.10$ for $\tau = 1$ and $M_N = 1.15$ and 1.20 for $\tau = 2$. For porosities of 3 and 6 percent, severe wave reflections are evident at most Mach numbers. Reference 4 concluded that the characteristics of this wall configuration at 6-percent porosity were similar to those of the conventional fixed 6-percent porosity, 60-deg inclined hole wall. However, the model pressure distribution at $M_N = 1.20$ in Fig. 12d does not support this conclusion. In fact, the present results indicate that walls A and B have similar characteristics and do not resemble the fixed-porosity wall characteristics.

The model pressure distributions obtained with upstream cutoff plate movement (wall C) at $\theta_w = 0$ are presented in Fig. 13. The distributions at $M_N = 0.95$ through 1.05 for $\tau = 0.5$ show wall interference in the form of a reflected compression from the shoulder expansion, implying that a smaller wall porosity would be beneficial, particularly at $M_N = 1.00$. However, there is little sensitivity to porosity in this Mach number range, as can be seen by comparing Figs. 13a, b, and c.

Structural considerations required that the cutoff plate be notched at the airside plate support points which resulted in several holes always

being open; the end effect was that the minimum wall porosity was 0.2 percent with all complete holes cut off. One check run was made at $\tau = 0.5$ with these open holes taped over, but the data did not show any conclusive effect on the reflected compression wave. However, it was noted that the open holes were producing local perturbations in the flow, and these perturbations can be seen in some of the model pressure distributions. For example, the open areas which influenced the model directly were located at model stations of x/d = 2.8, 6.5, and 10.1. The data in Fig. 13a show a perturbation at x/d = 6.5 for $M_N = 1.00$ and again at x/d = 7.4 for $M_N = 1.05$ which, from Fig. 10, is the expected downstream displacement with Mach number.

The model pressure distribution at $M_N = 1.05$ with $\tau = 1$ (Fig. 13b) is the closest to interference-free data obtained in the present study for this Mach number. The reflected disturbances obtained with walls A and B were considerably reduced in magnitude with wall C.

Similar reductions of wall interference were obtained with wall C at higher Mach numbers. Specifically, $M_N = 1.10$ at $\tau = 2$, $M_N = 1.15$ at $\tau = 3$, and $M_N = 1.20$ at $\tau = 6$ show practically no wall interference. In fact, the quoted distributions at $M_N = 1.10$ and 1.15 represent the most nearly interference-free data published for a cone-cylinder model of near 1-percent blockage.

In an attempt to eliminate the shoulder-induced compression at $M_N = 1.0$, walls D, E, and F were tested. The model pressure distributions with these walls are presented in Figs. 14 through 16. No improvement over wall C was obtained.

4.3 INFLUENCE OF WALL ANGLE

The effects of wall angle variation upon the model pressure distributions obtained with wall C are shown in Fig. 17. In general, converging the test section walls is roughly equivalent to decreasing the wall porosity. This is particularly evident in Fig. 17e by comparing the data at $\tau = 3$ and $\theta_w = 0$ with that for $\tau = 6$ and $\theta_w = -0.5$.

Wall angle variations appear to have more effect on the model pressure distributions at the lower wall porosities, but the data are not conclusive. The issue is clouded by the fact that the Mach number settings were less precise at the lower wall porosities. However, the calibration data of Ref. 5 do show that the wall pressure differential is more sensitive to wall angle changes at low wall porosity than at high porosity. The end result is that it may be possible to improve upon the

best model pressure distributions obtained here utilizing wall angle variation as a supplement to wall porosity variation.

For the present tests, the model pressure distributions obtained with variable wall angle are not significantly improved relative to the zero wall angle distributions. However, the optimum combinations of wall angle and wall porosity were not tested.

4.4 COMPARISON OF FIXED AND VARIABLE POROSITY

The AEDC-PWT 16-Foot Transonic Tunnel (Tunnel 16T) is equipped with conventional perforated test section walls (60-deg inclined holes, fixed 6-percent porosity), and data from a 20-deg cone-cylinder model of 1-percent blockage in this tunnel are presented in Ref. 8.

The optimum results of the present study are compared in Fig. 18 with data from Tunnel 16T (Ref. 8) at $\theta_W = 0$. Significant reduction of the wave reflection interference is shown at $M_N = 1.05$ and 1.10 with the variable porosity wall. Both the fixed and the variable wall are equally effective at $M_N = 1.20$.

SECTION V
CONCLUSIONS

An experimental investigation of the wall-interference effects on a 20-deg cone-cylinder model has been conducted in the Mach range from 0.95 to 1.20 in conjunction with various variable perforated test section walls. The data obtained during this investigation are summarized as follows:

1. Upstream movement of the sliding plates provides a test section boundary which successfully minimizes wave reflection wall interference throughout most of the transonic range.
2. Significant reductions in wall interference effects are obtained with the variable porosity test section relative to the conventional fixed porosity walls.
3. Wall angle and wall porosity variations have similar effects upon the wave cancellation characteristics of the variable porosity wall with upstream cutoff plate movement.
4. The 1-ft transonic tunnel equipped with variable porosity test section walls has proved to be an adequate working model of the 4-ft transonic tunnel.

REFERENCES

1. Estabrooks, Bruce B. "Wall-Interference Effects on Axisymmetric Bodies in Transonic Wind Tunnels." AEDC-TR-59-12 (AD216698), June 1959.

2. Simon, Erwin. "Calibration Tests of the MSFC 14 x 14-Inch Trisonic Wind Tunnel." NASA TMX-53113, August 1964.

3. Hartley, M. S. and Jacocks, J. L. "Initial Calibration Results from the AEDC-PWT 4-Foot Transonic Tunnel." AEDC-TR-68-141 (AD837078), August 1968.

4. Jacocks, J. L. and Banks, M. R. "Cross-Flow Characteristics of Variable-Porosity Perforated Plates at Mach Numbers from 0.9 to 1.2." AEDC-TR-69-33 (AD847674), February 1969.

5. Jackson, F. M. "Calibration of the AEDC-PWT 1-Ft Transonic Tunnel with Variable Porosity Test Section Walls." AEDC-TR-69-114, to be published.

6. Test Facilities Handbook (Seventh Edition). "Propulsion Wind Tunnel Facility, Vol. 5." Arnold Engineering Development Center, July 1968.

7. Hartley, M. S. and Jacocks, J. L. "Static Pressure Distributions on Various Bodies of Revolution at Mach Numbers from 0.60 to 1.60." AEDC-TR-68-37 (AD828571), March 1968.

8. Nichols, James H. "Determination of Optimum Operating Parameters for the PWT 16-Ft Transonic Circuit Utilizing One-Percent Bodies of Revolution." AEDC-TN-59-100 (AD225362), September 1959.

APPENDIX
ILLUSTRATIONS

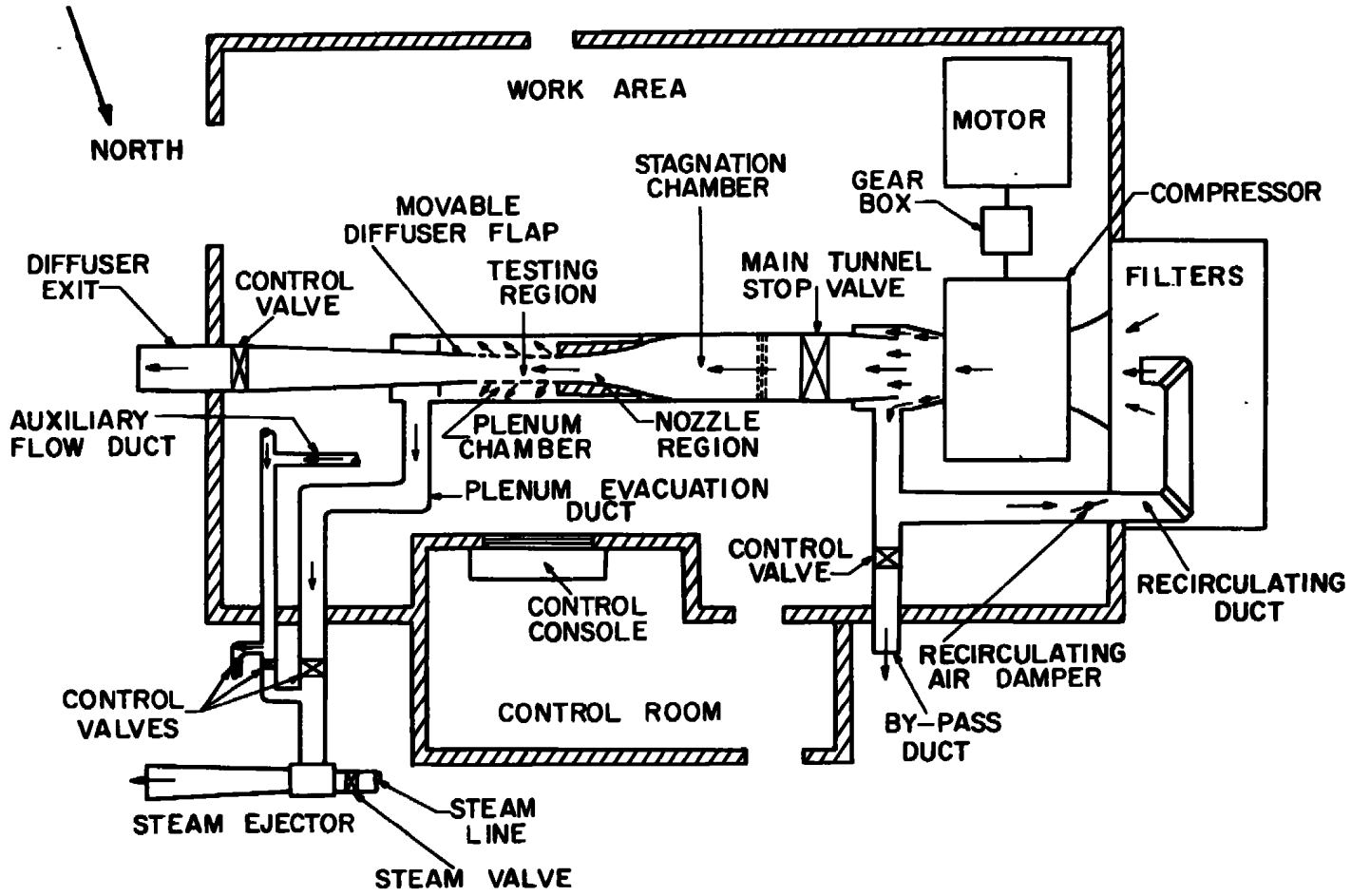

Fig. 1 Layout of Tunnel 1T

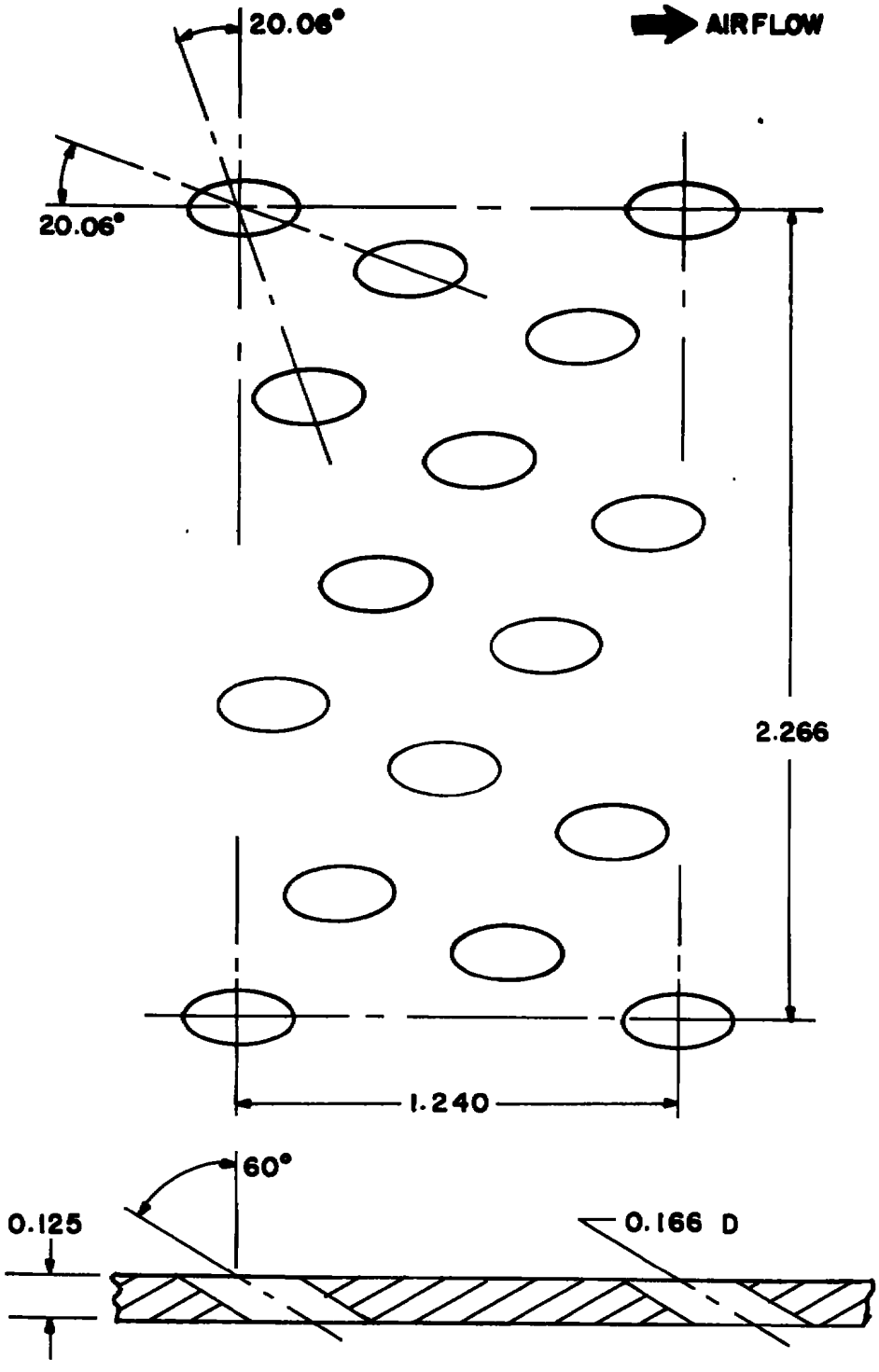

Fig. 2 Airside Wall Geometry

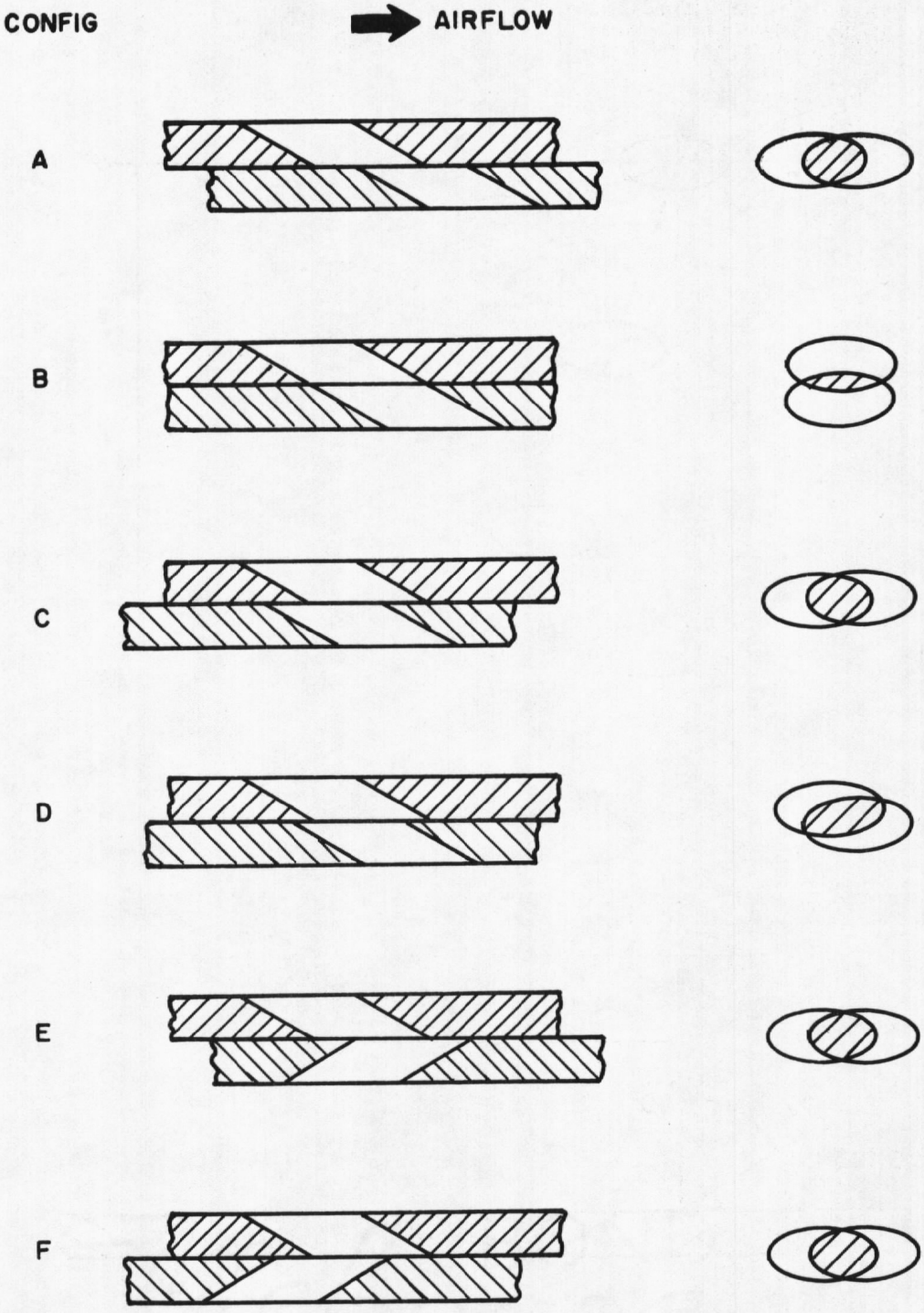

Fig. 3 Cutoff Plate Geometry and Wall Configuration Designations

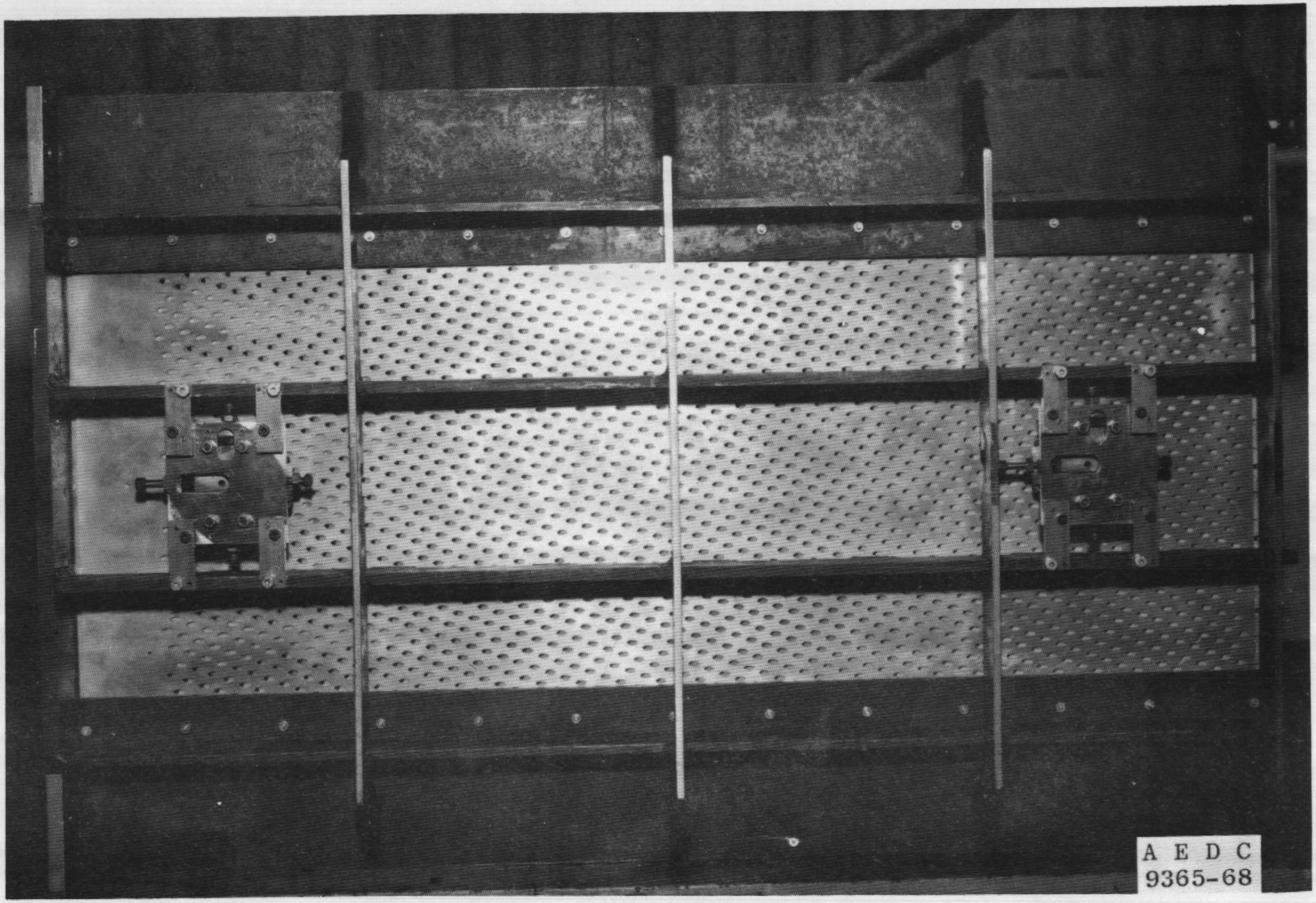

Fig. 4 Photograph of Back of South Test Section Wall

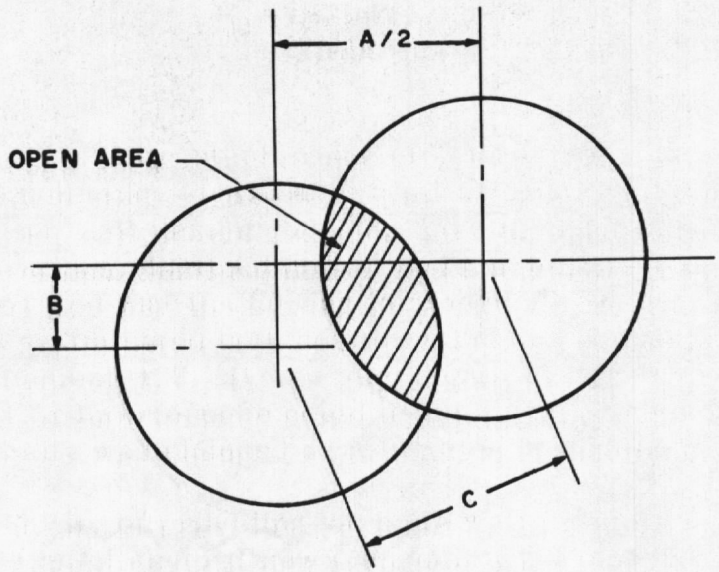

VIEW ALONG AIRSIDE HOLE AXIS

A = LONGITUDINAL CUTOFF PLATE TRAVEL, IN.

B = TRANSVERSE CUTOFF PLATE TRAVEL, IN.

$$C = \left[\frac{A^2}{4} + B^2\right]^{1/2} \qquad D = 0.166 \text{ IN.}$$

$$\tau = \frac{20}{\pi}\left\{\cos^{-1}\frac{C}{D} - \frac{C}{D}\left[1 - \left(\frac{C}{D}\right)^2\right]^{1/2}\right\}$$

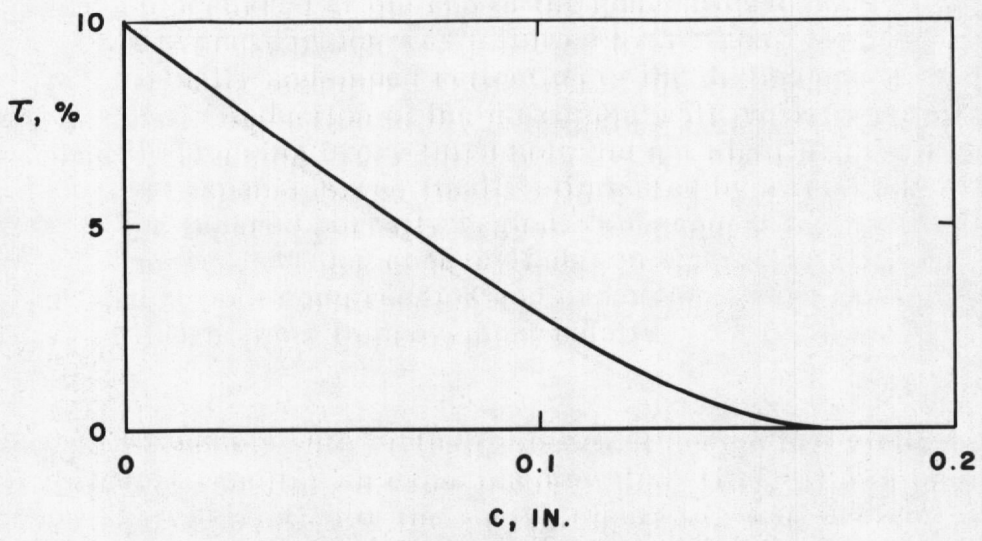

Fig. 5 Wall Porosity and Cutoff Plate Travel Relationship

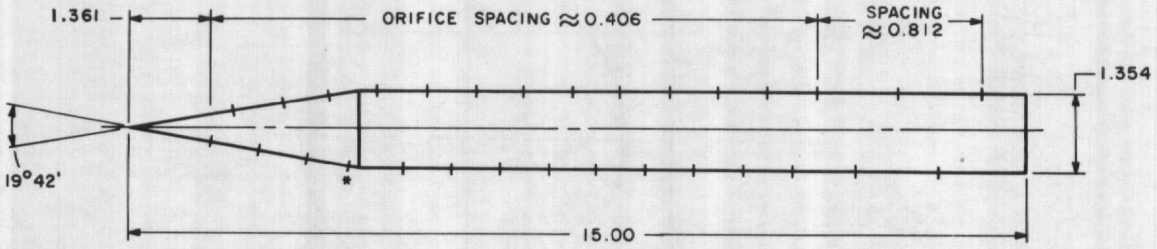

* ORIFICE SHIFTED UPSTREAM 0.135
ALL DIMENSIONS IN INCHES

ORIFICE LOCATIONS

BOTTOM ROW NO.	x/d	TOP ROW NO.	x/d
1	1.005	2	1.304
3	1.606	4	1.905
5	2.205	6	2.504
7	2.699	8	3.095
9	3.398	10	3.700
11	3.999	12	4.300
13	4.598	14	4.900
15	5.199	16	5.498
17	5.798	18	6.099
19	6.397	20	6.699
21	6.999	22	7.299
23	7.600	24	7.901
25	8.198	26	8.498
27	8.997	28	9.500
29	9.996	30	10.496

Fig. 6 Sketch of 20-deg Cone-Cylinder Model

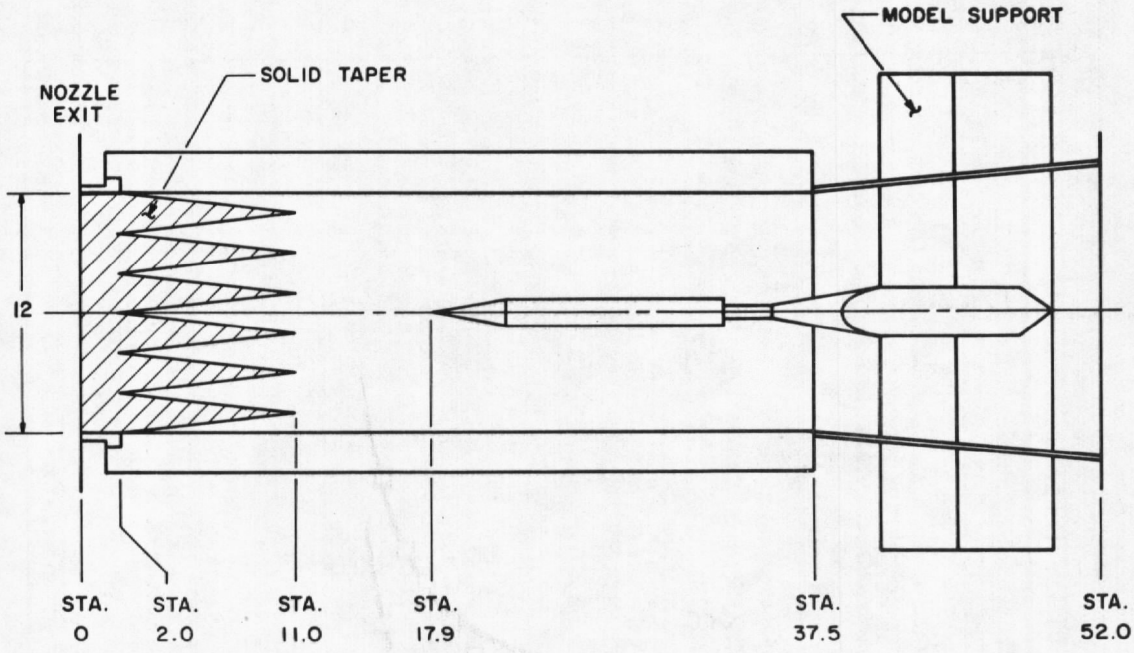

Fig. 7 Sketch of Tunnel 1T Test Section

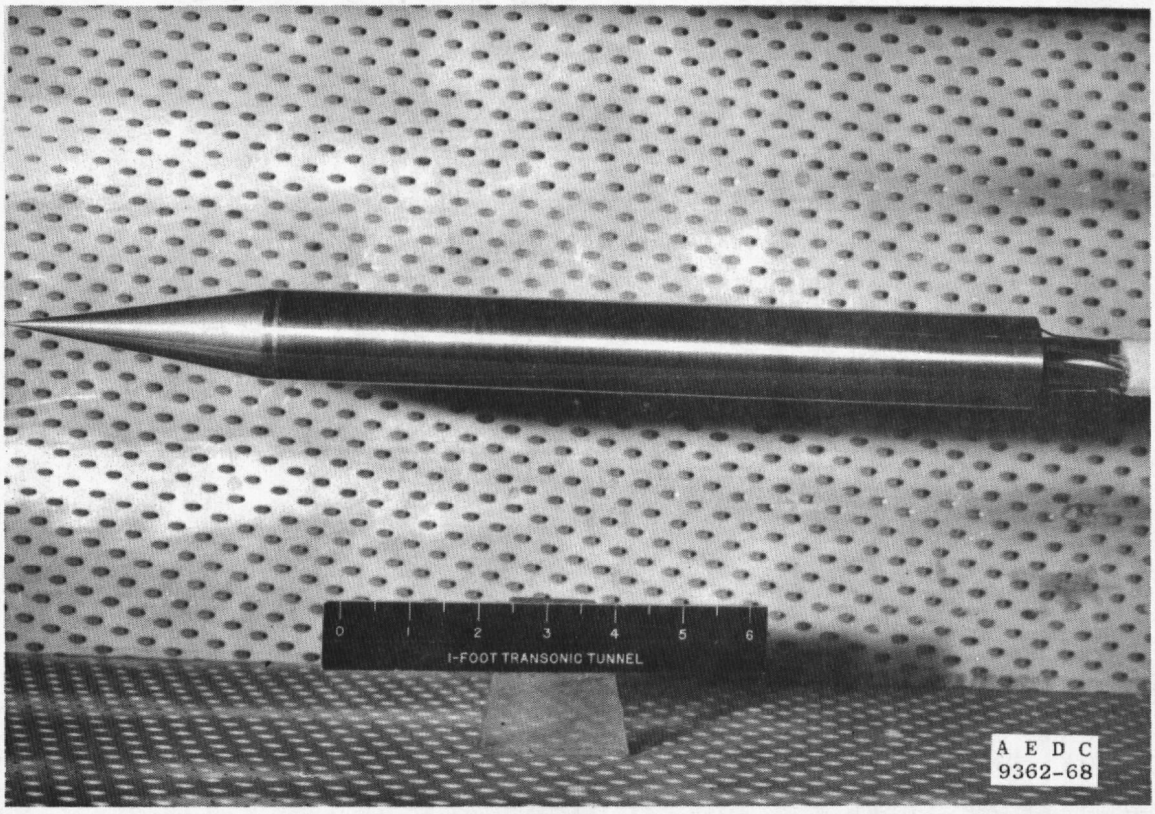

Fig. 8 Photograph of 20-deg Cone-Cylinder Model Installation

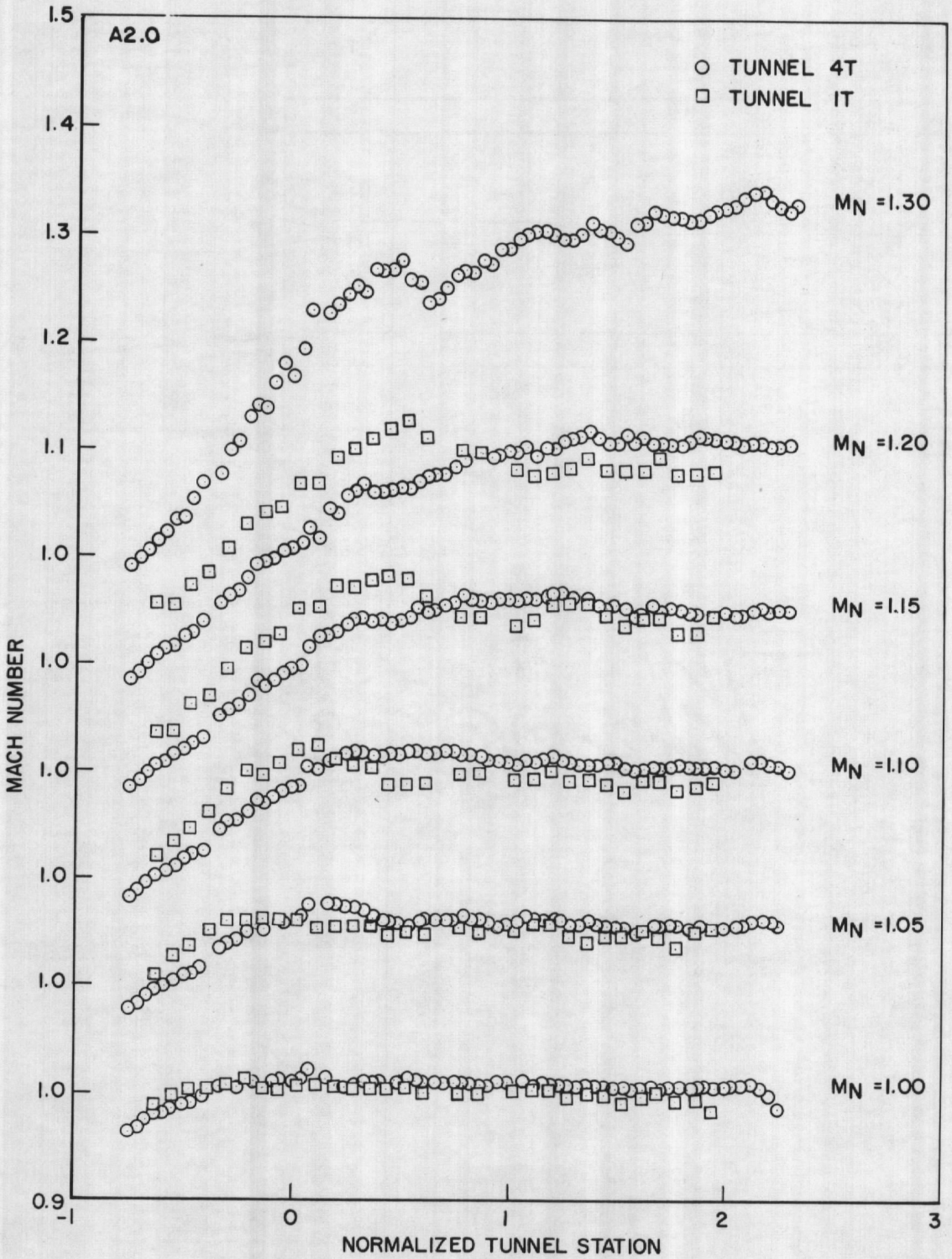

a. τ = 2.0

Fig. 9 Comparison of the Centerline Mach Number Distributions in Tunnel 1T and 4T, Wall A, θ_w = 0

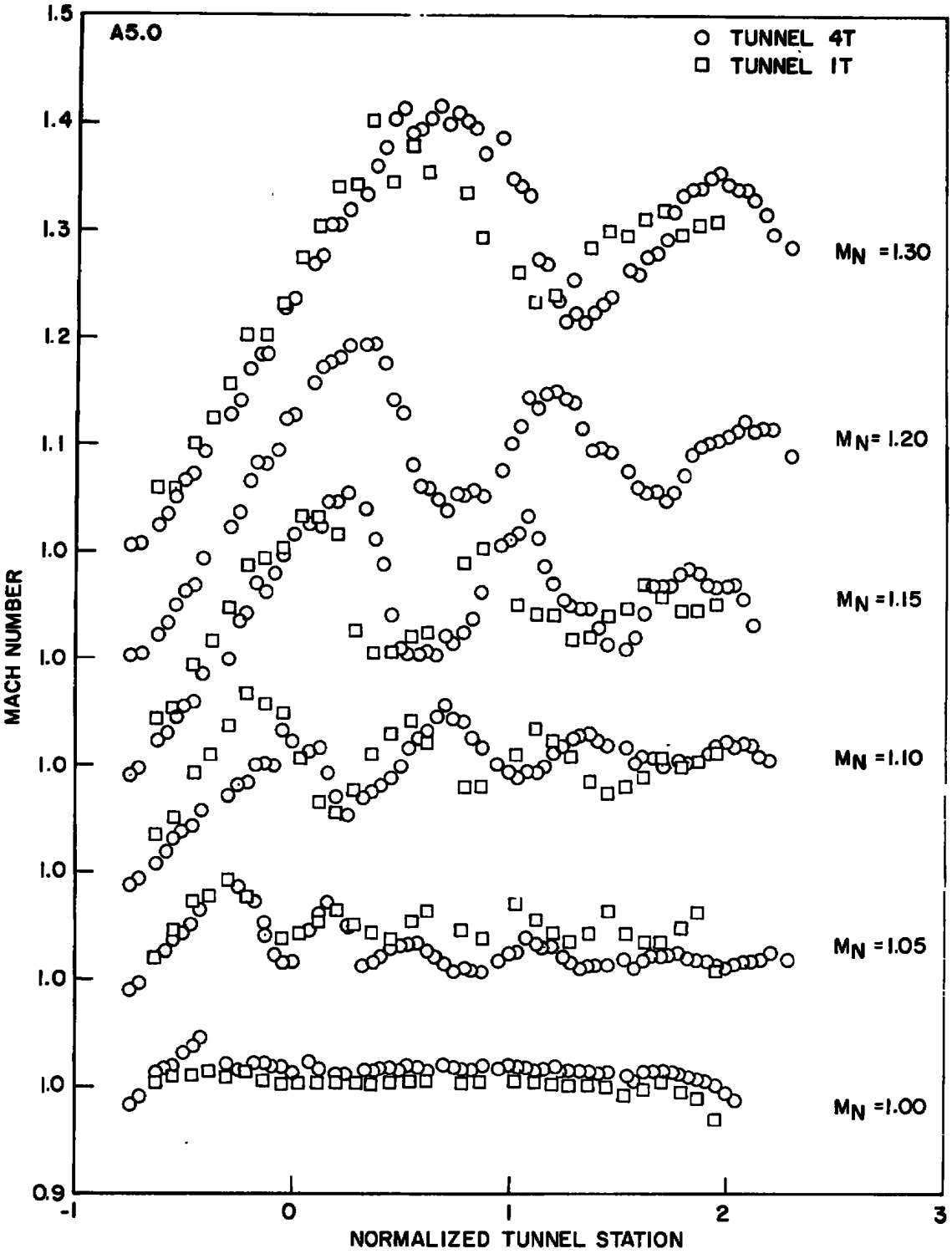

b. τ = 5.0

Fig. 9 Concluded

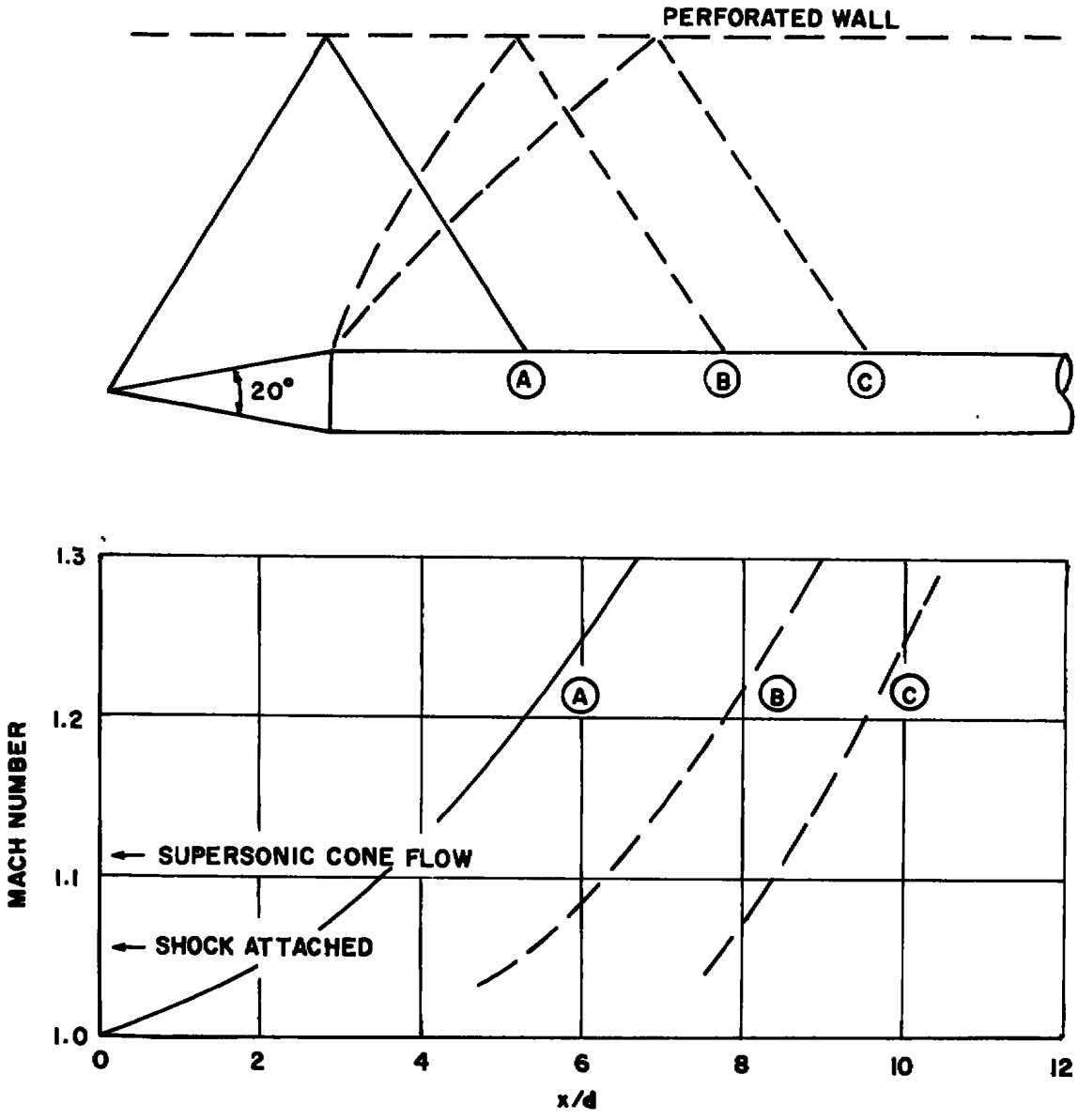

Fig. 10 Approximate Locations of Reflected Wave Disturbances upon a 1-percent Blockage, 20-deg Cone-Cylinder Model

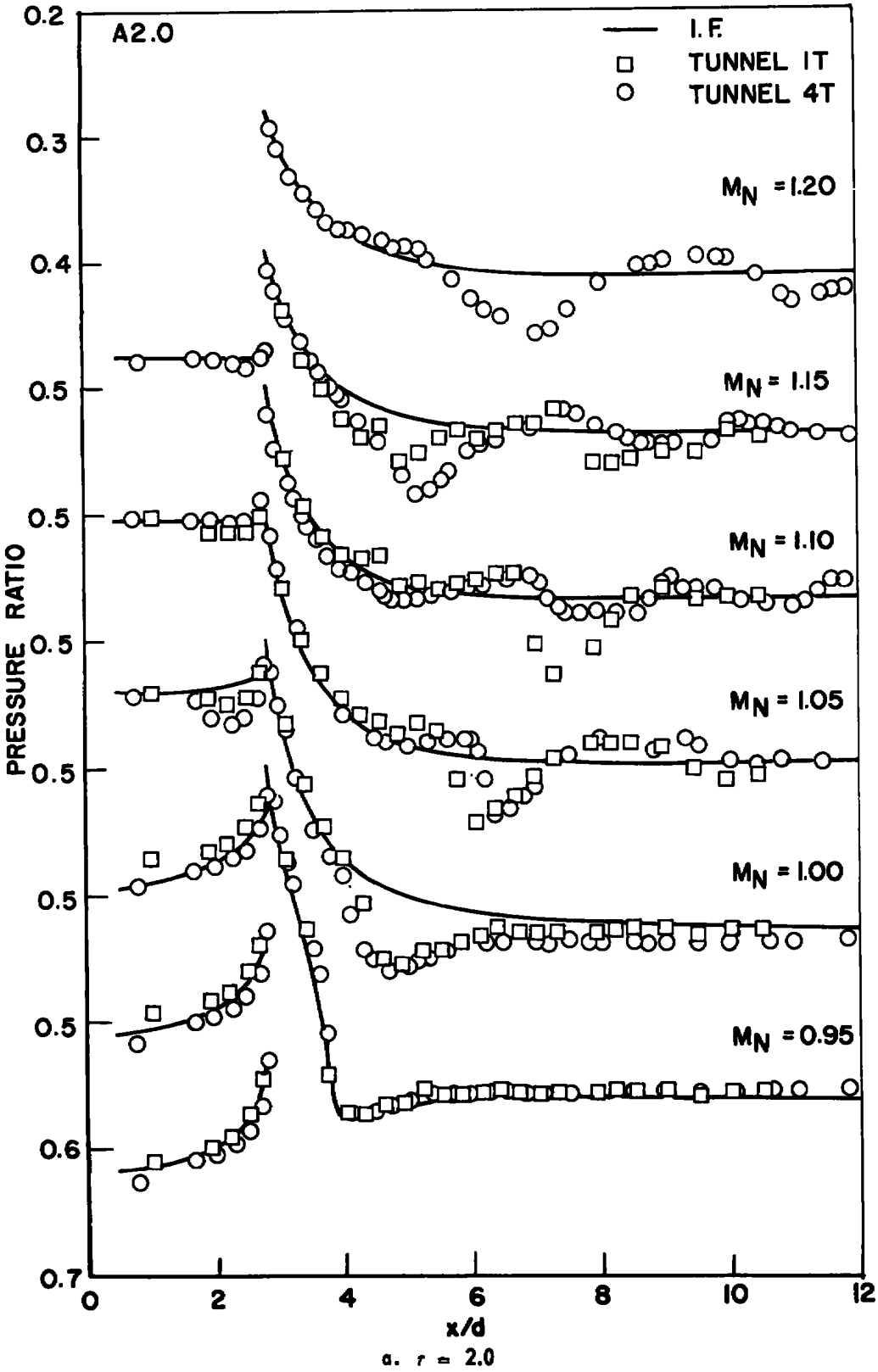

a. $r = 2.0$

Fig. 11 Comparison of the Model Pressure Distributions in Tunnels 1T and 4T, Wall A, $\theta_w = 0$

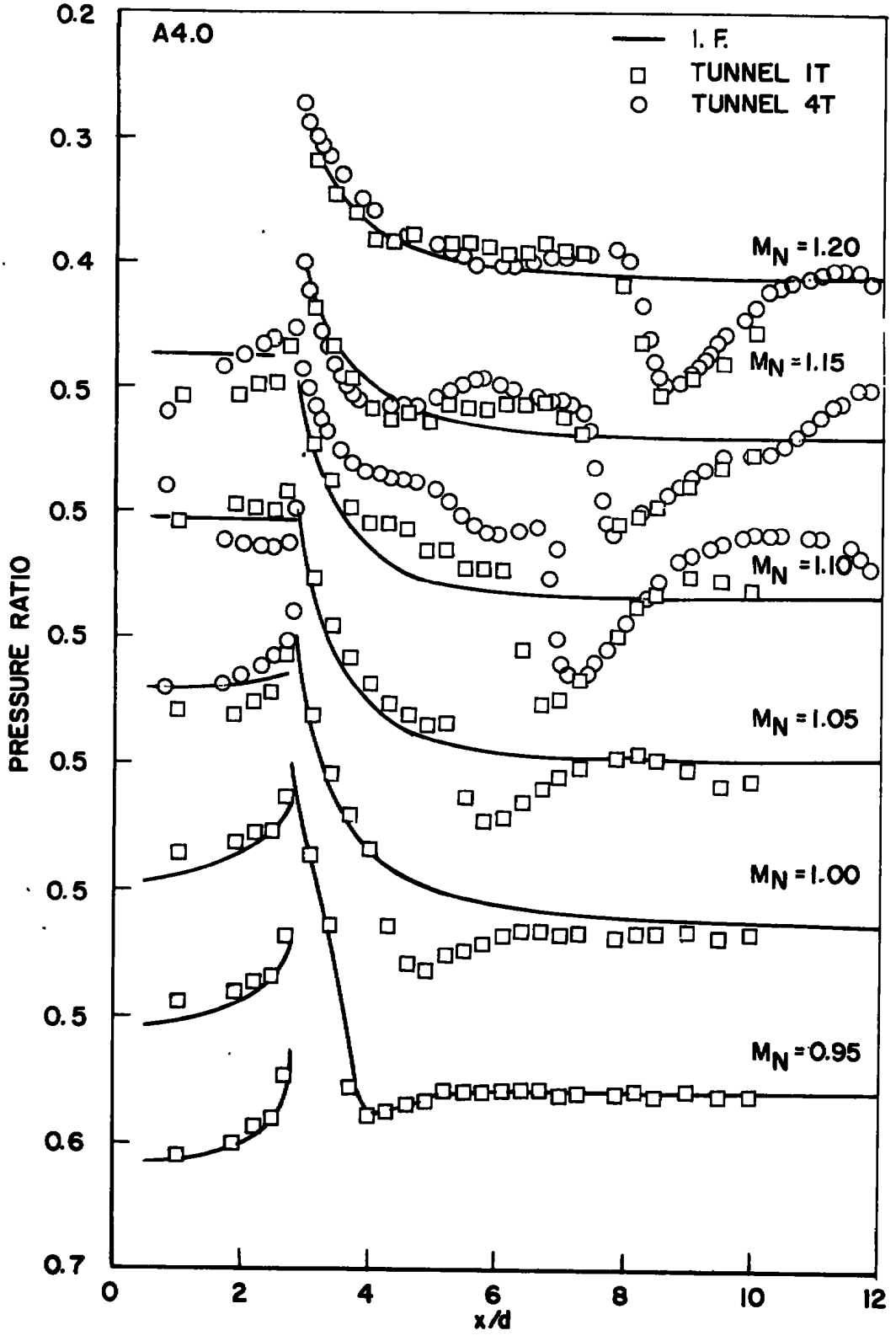

b. r = 4.0

Fig. 11 Concluded

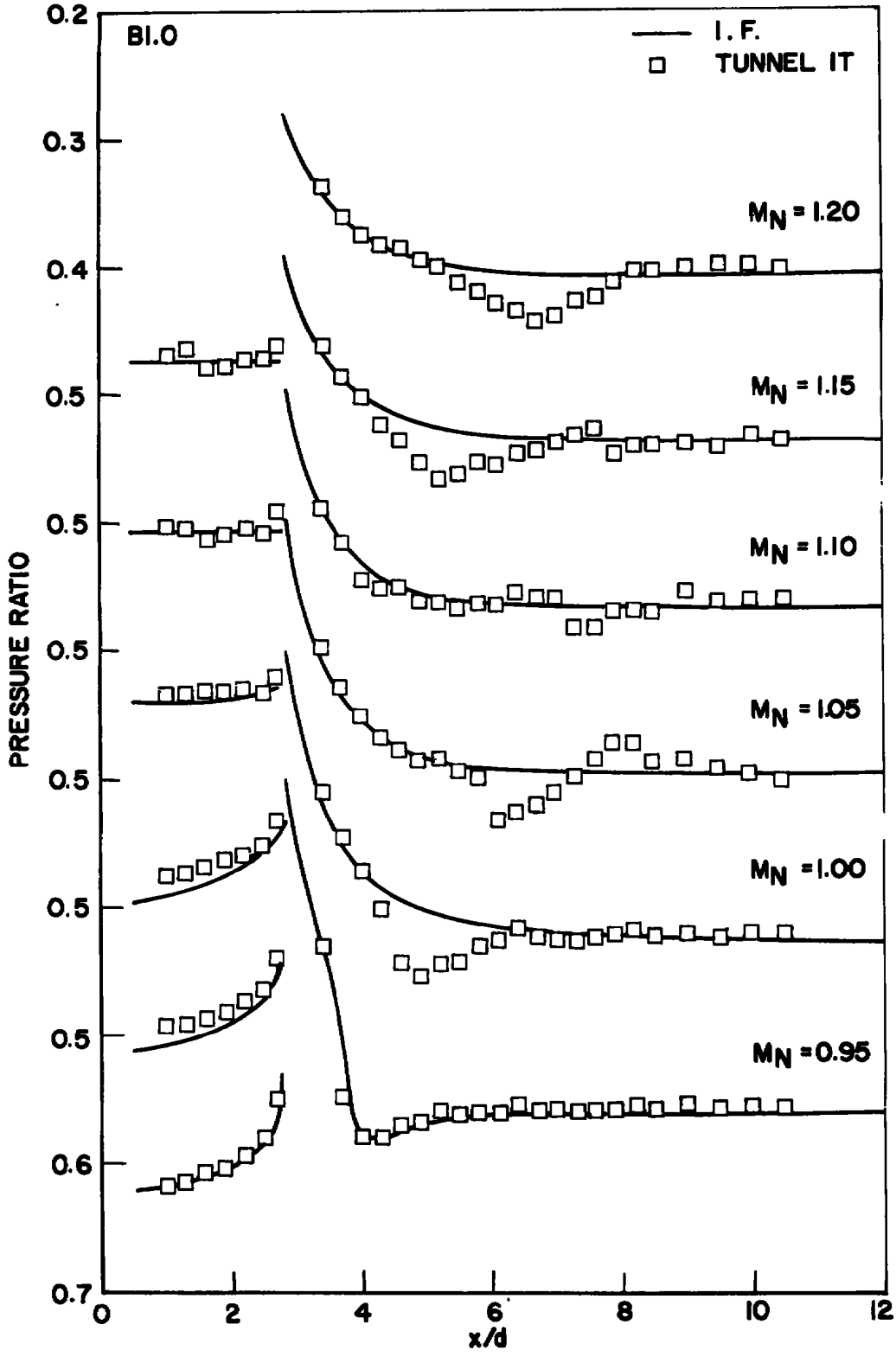

a. r = 1.0

Fig. 12 Model Pressure Distributions with Wall B, θ_w = 0

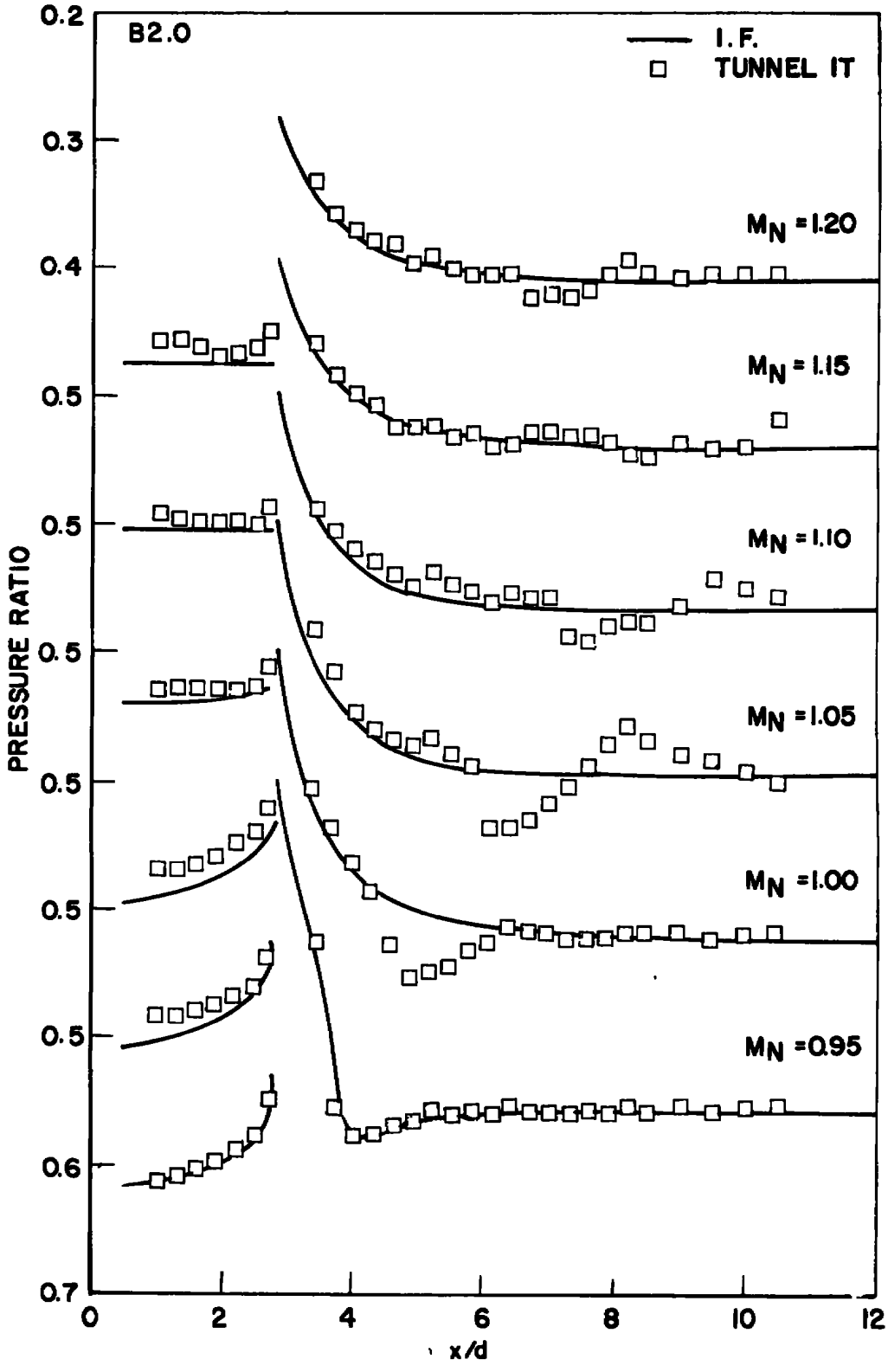

b. r = 2.0

Fig. 12 Continued

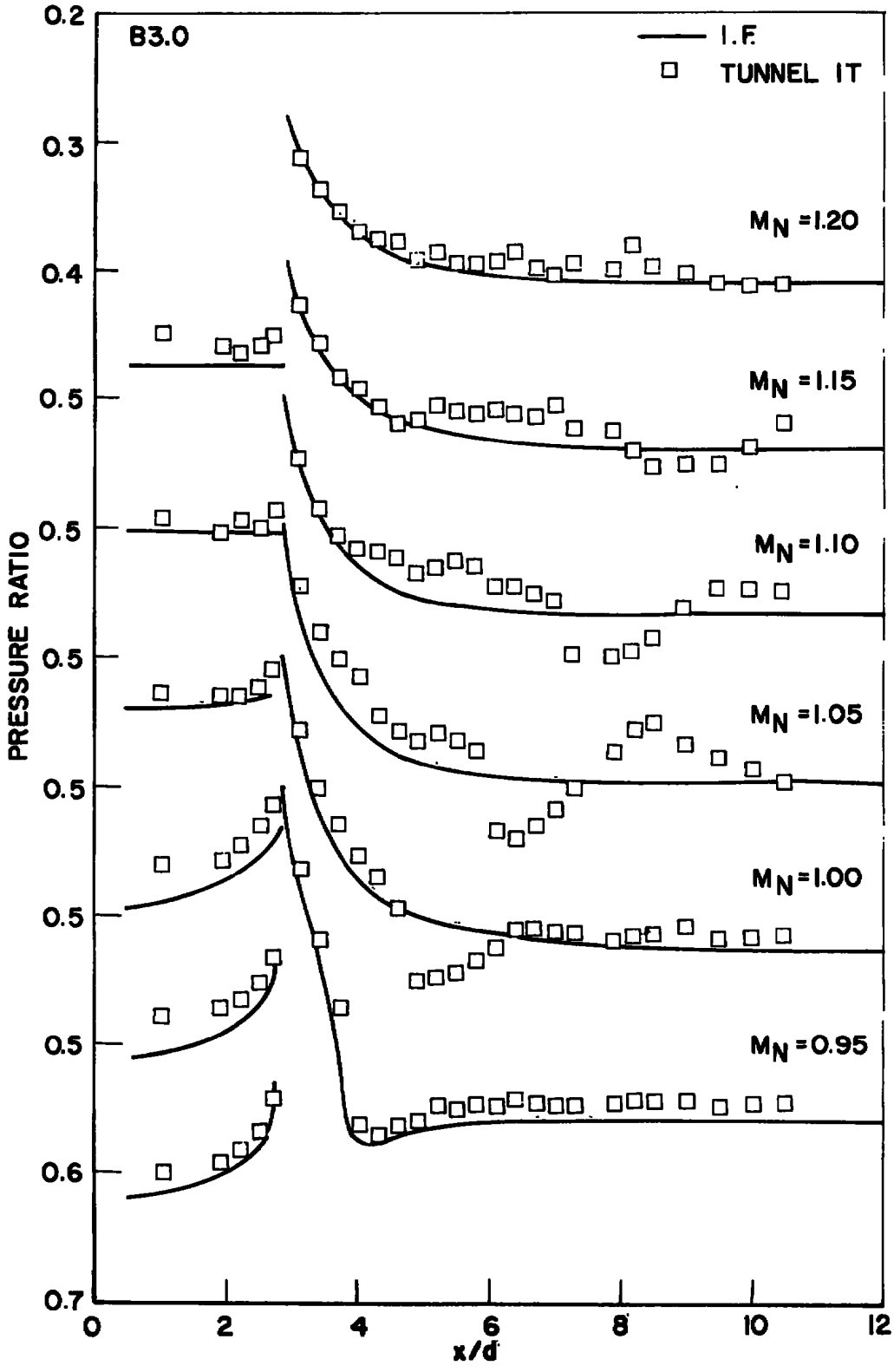

c. r = 3.0

Fig. 12 Continued

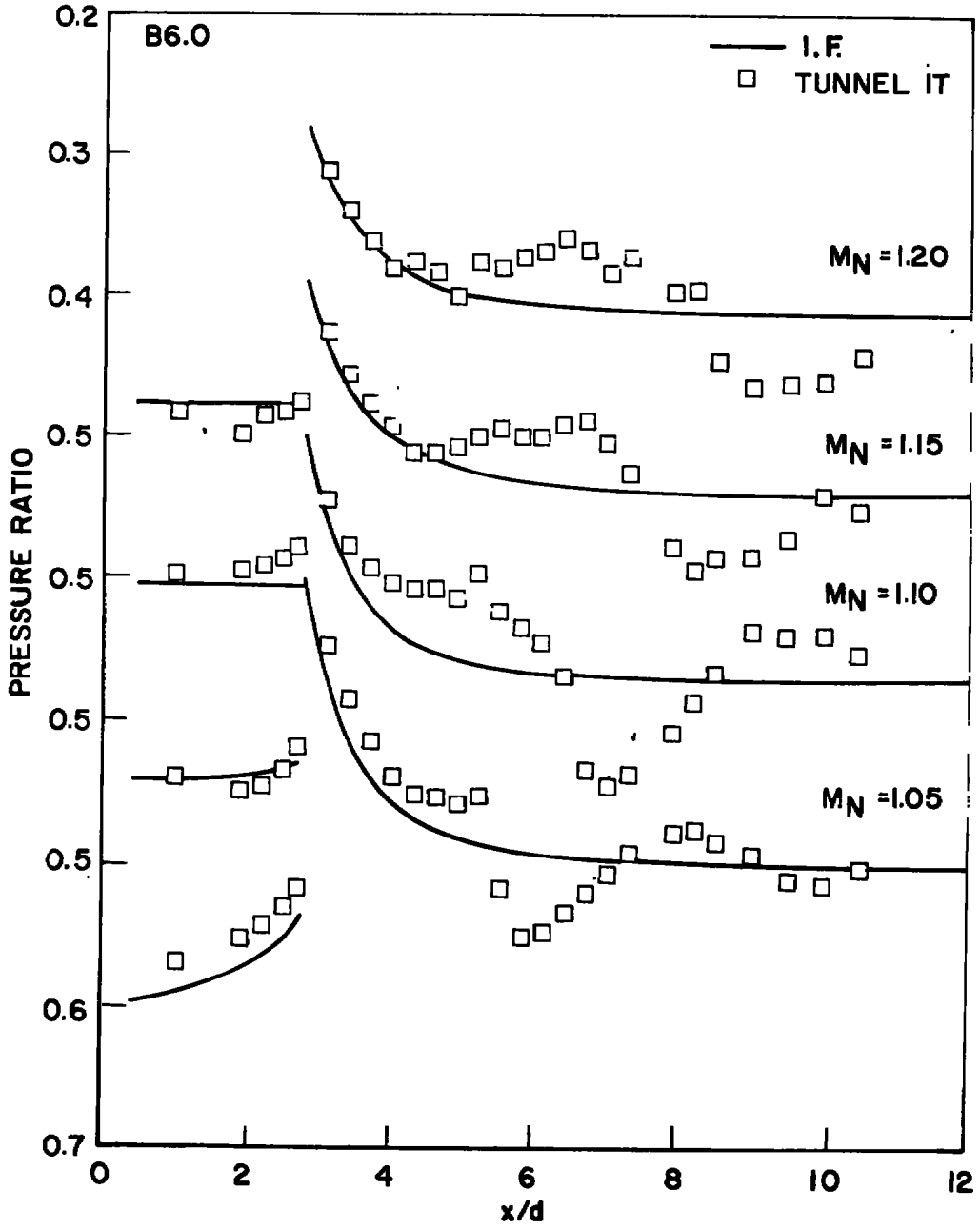

d. r = 6.0

Fig. 12 Concluded

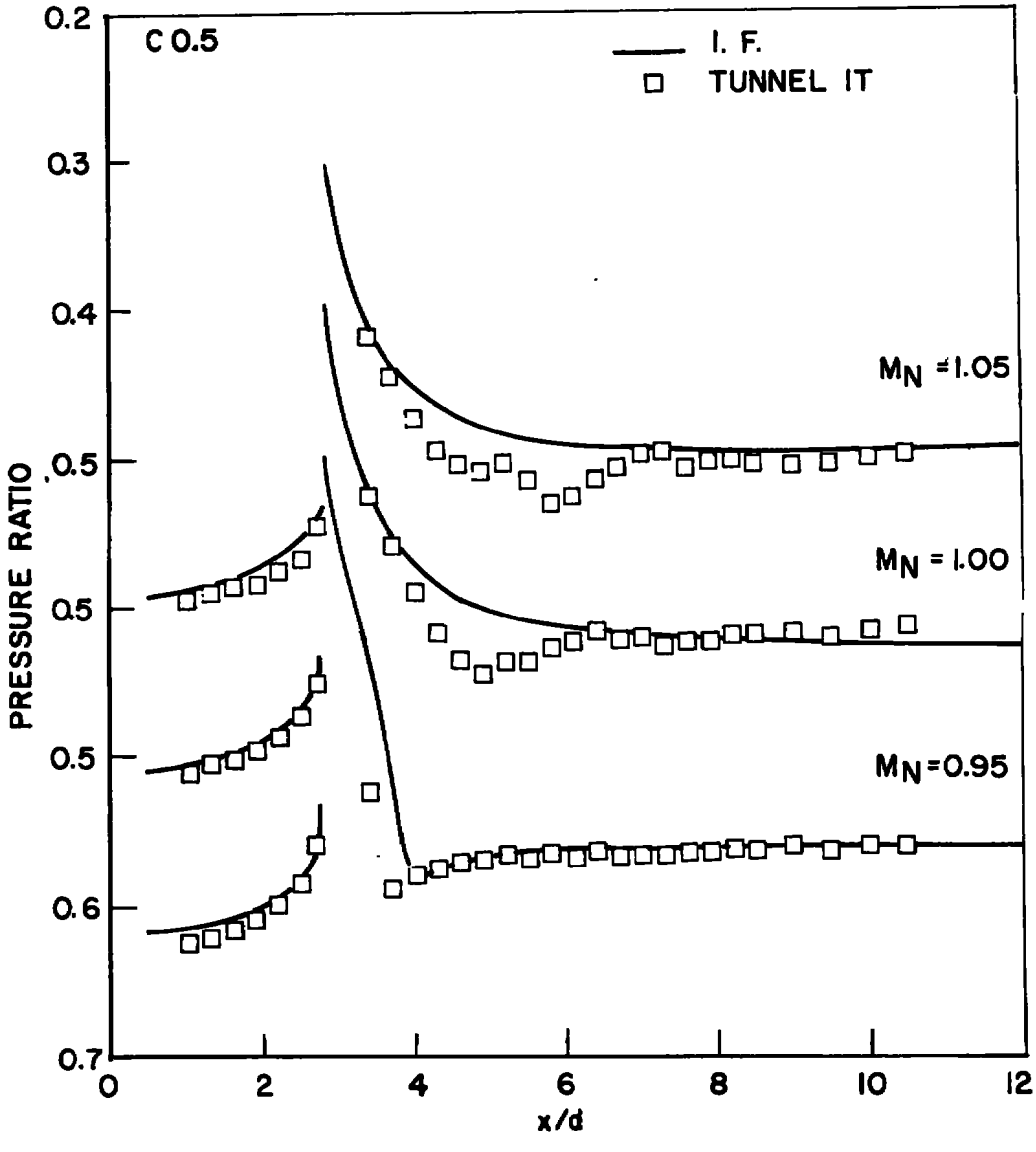

a. τ = 0.5

Fig. 13 Model Pressure Distributions with Wall C, θ_w = 0

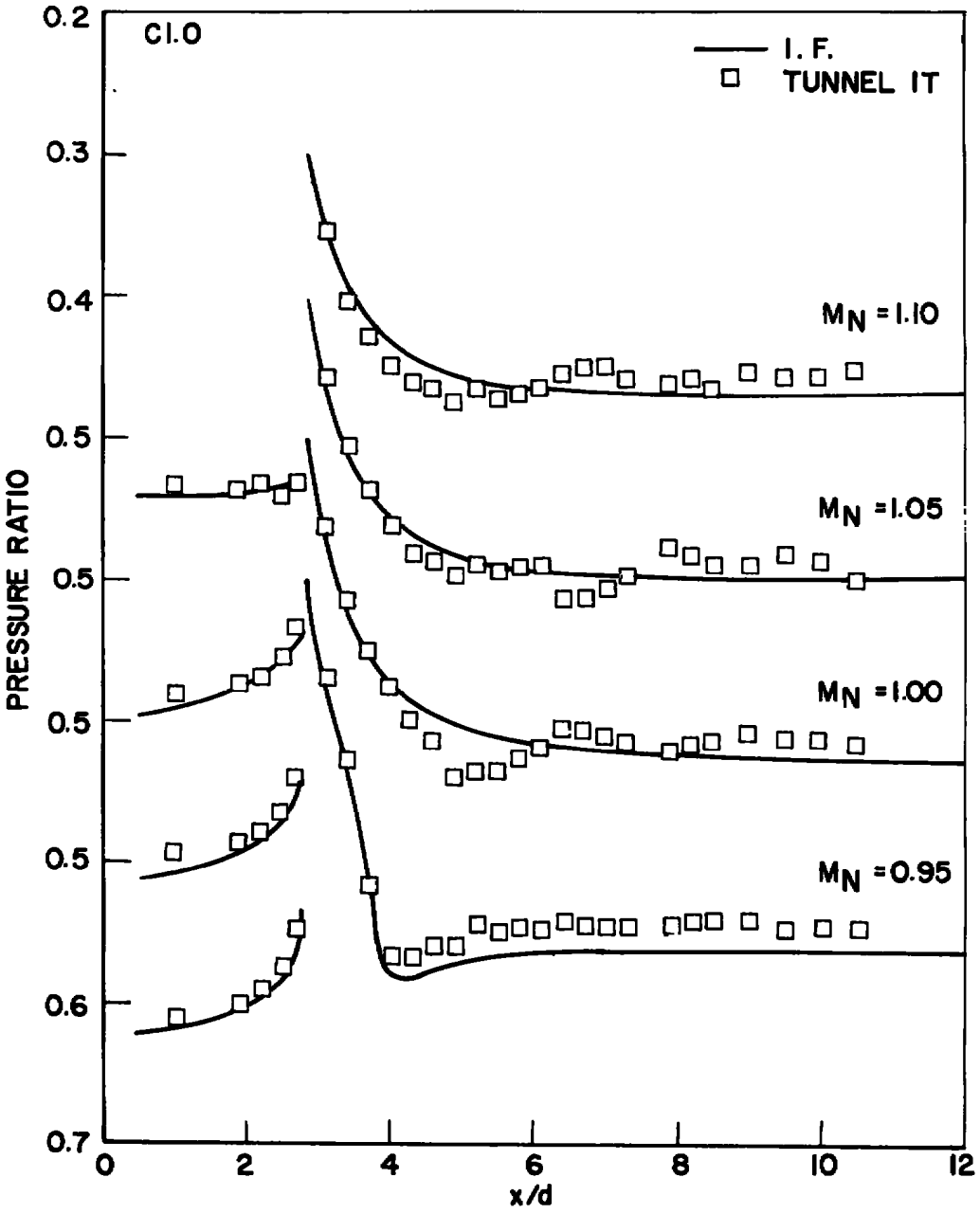

b. r = 1.0

Fig. 13 Continued

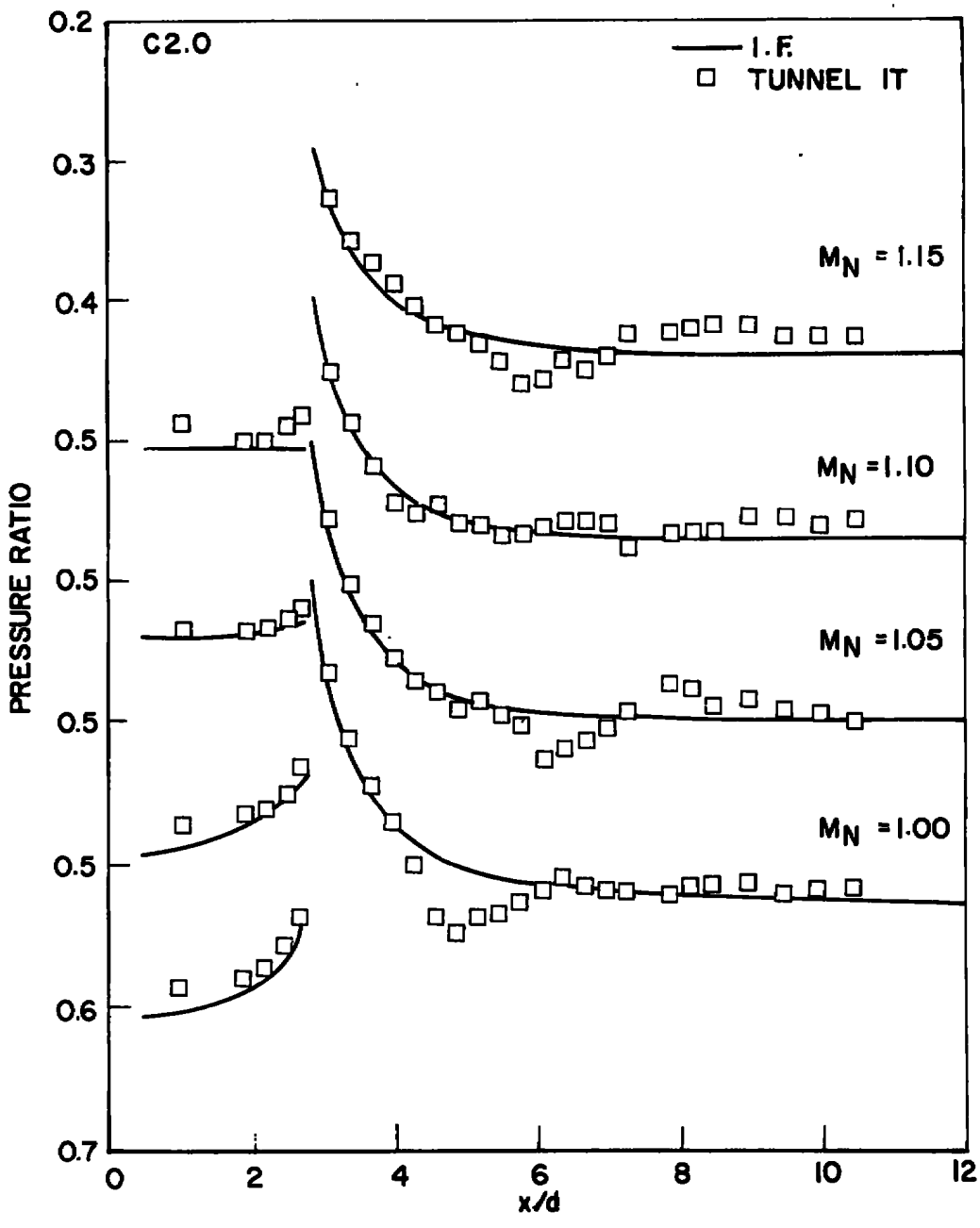

c. r = 2.0

Fig. 13 Continued

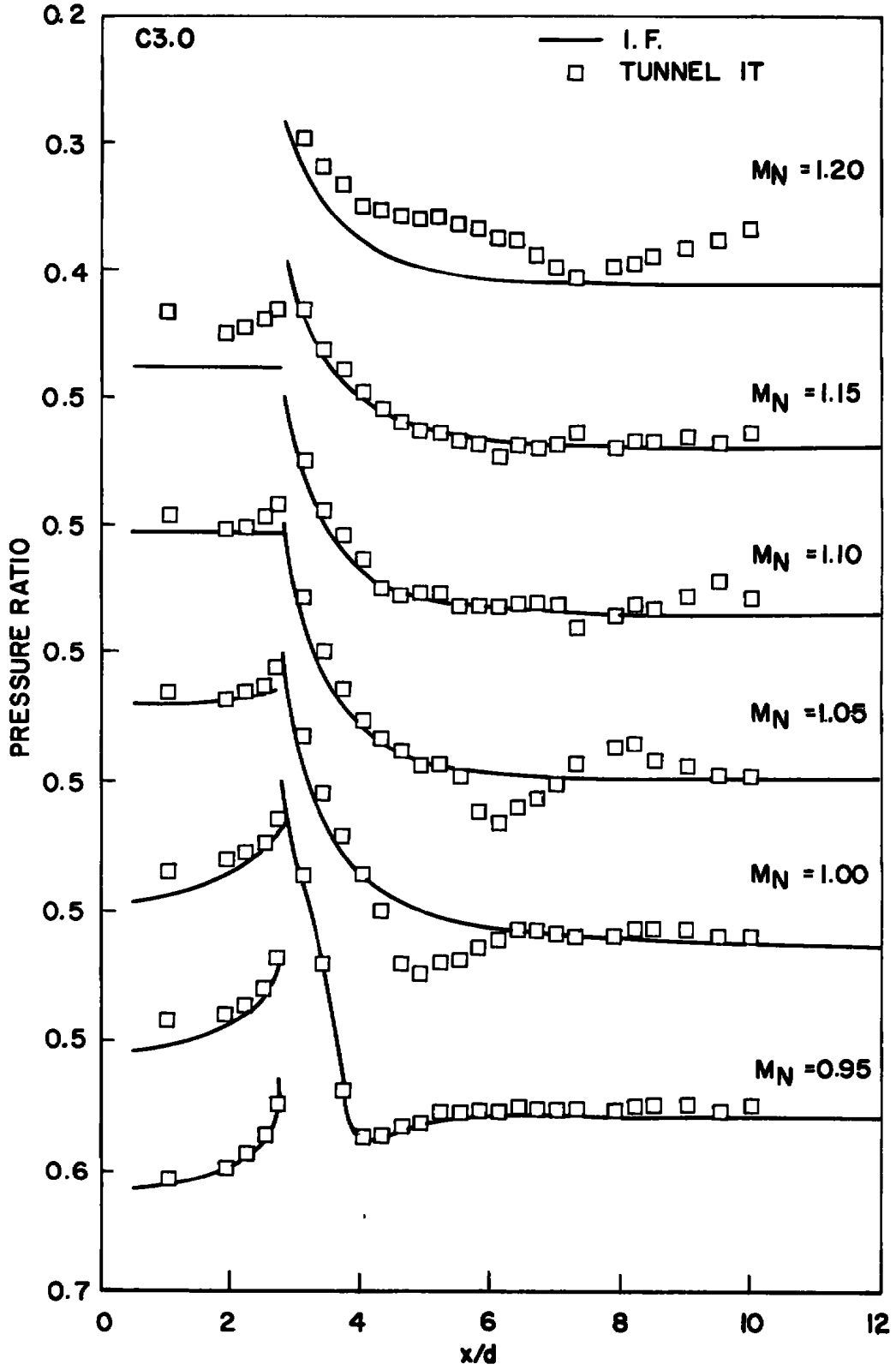

d. r = 3.0

Fig. 13 Continued

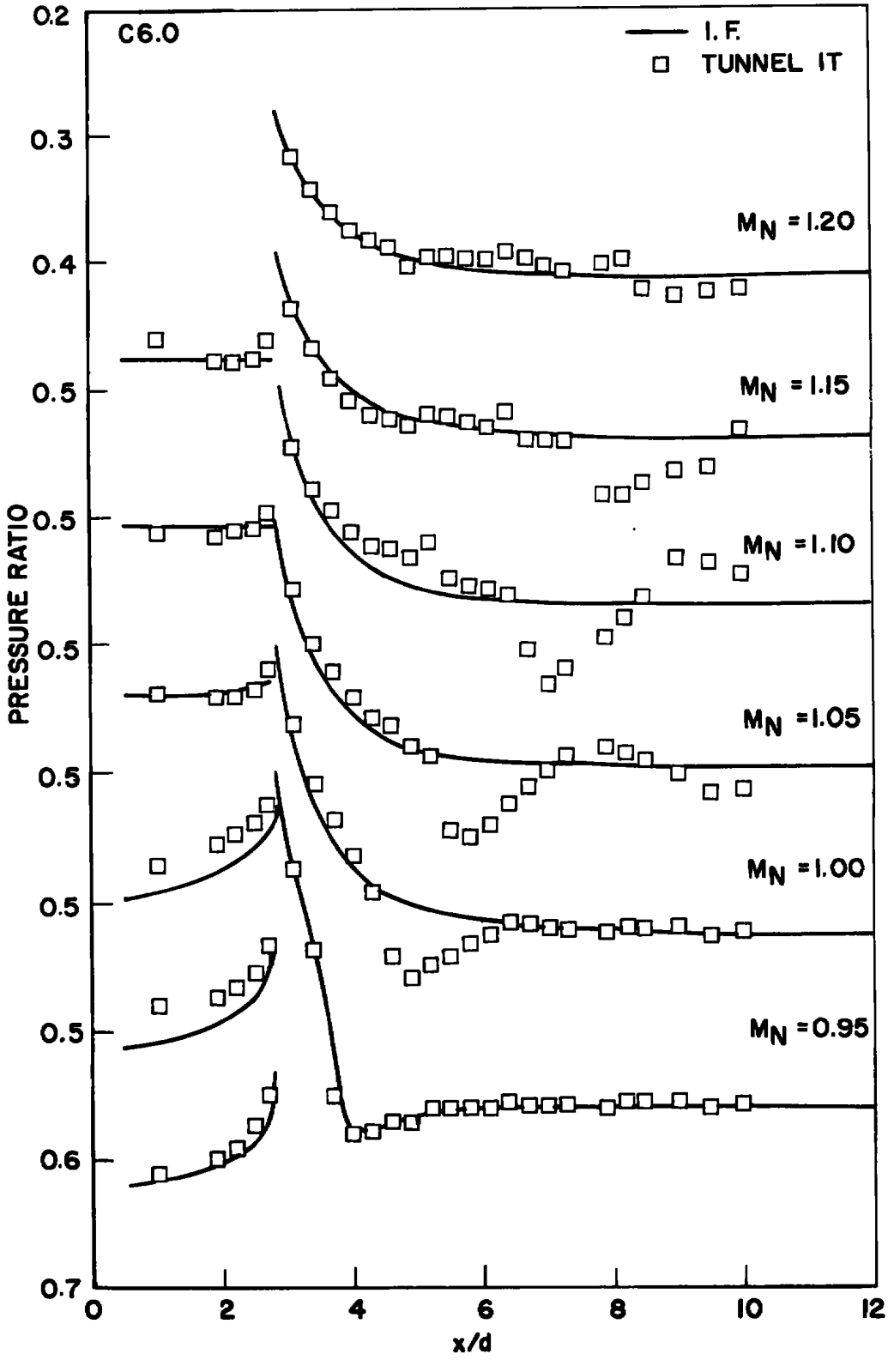

e. τ = 6.0

Fig. 13 Concluded

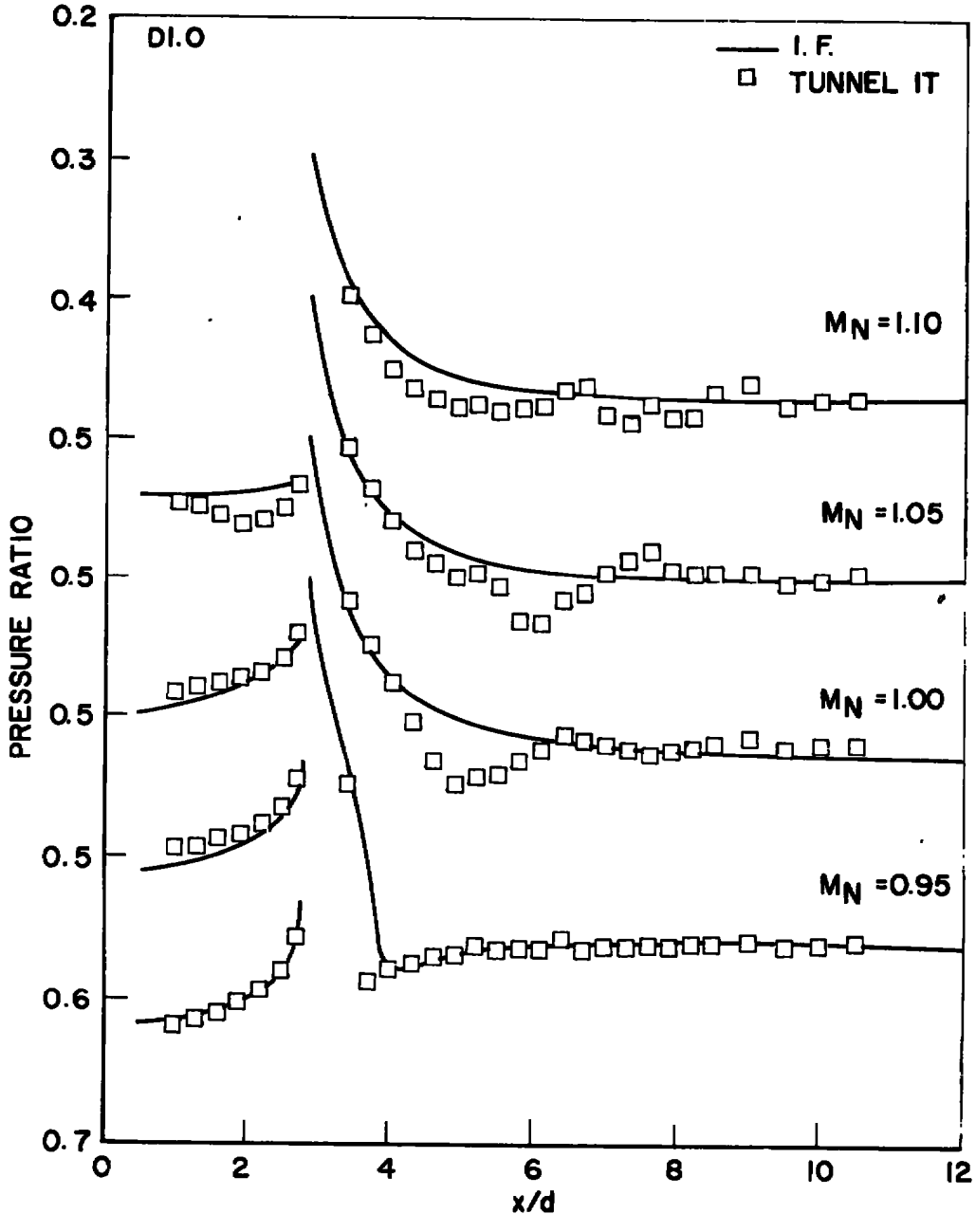

Fig. 14 Model Pressure Distributions with Wall D, $\theta_w = 0$, $r = 1.0$

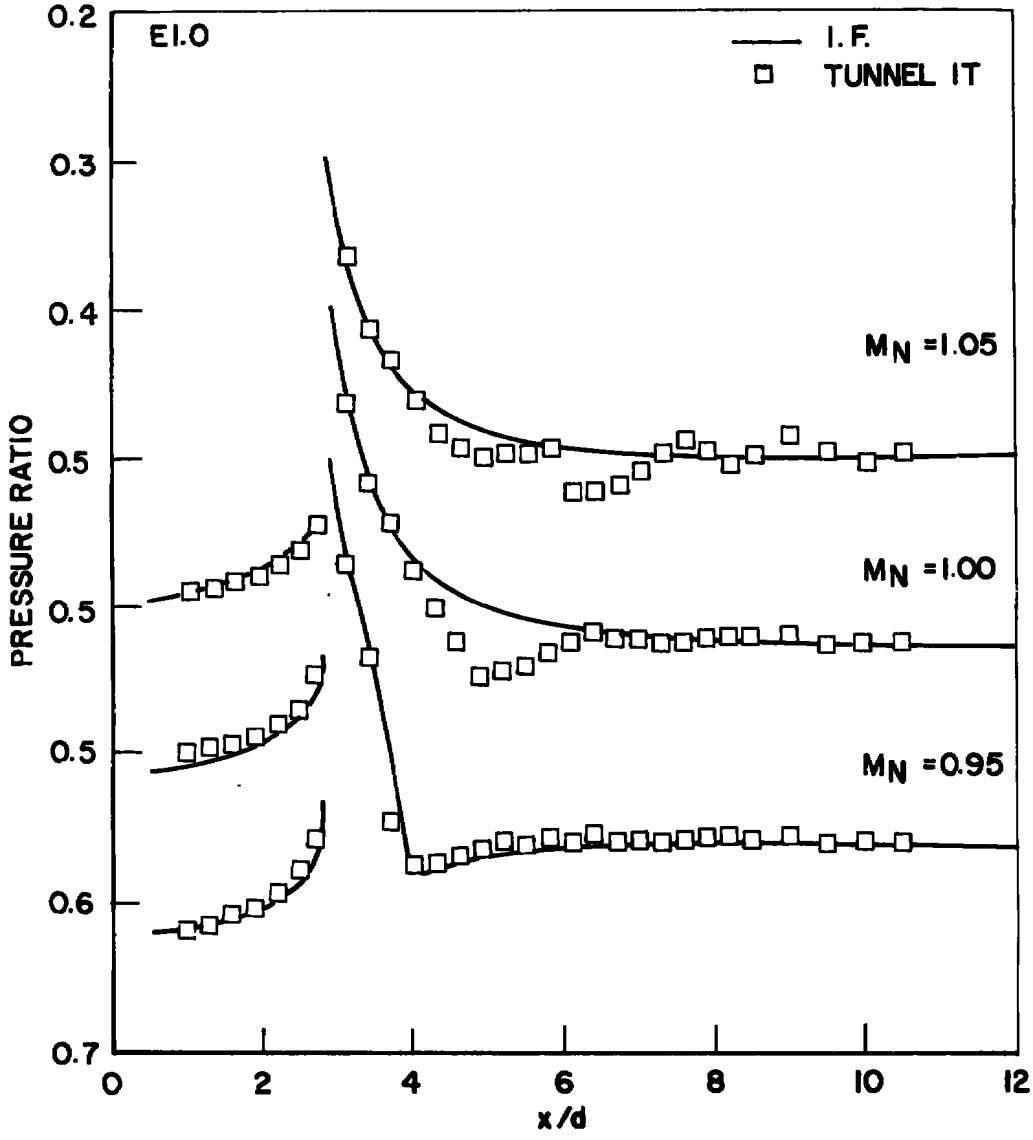

a. r = 1.0

Fig. 15 Model Pressure Distributions with Wall E, θ_w = 0

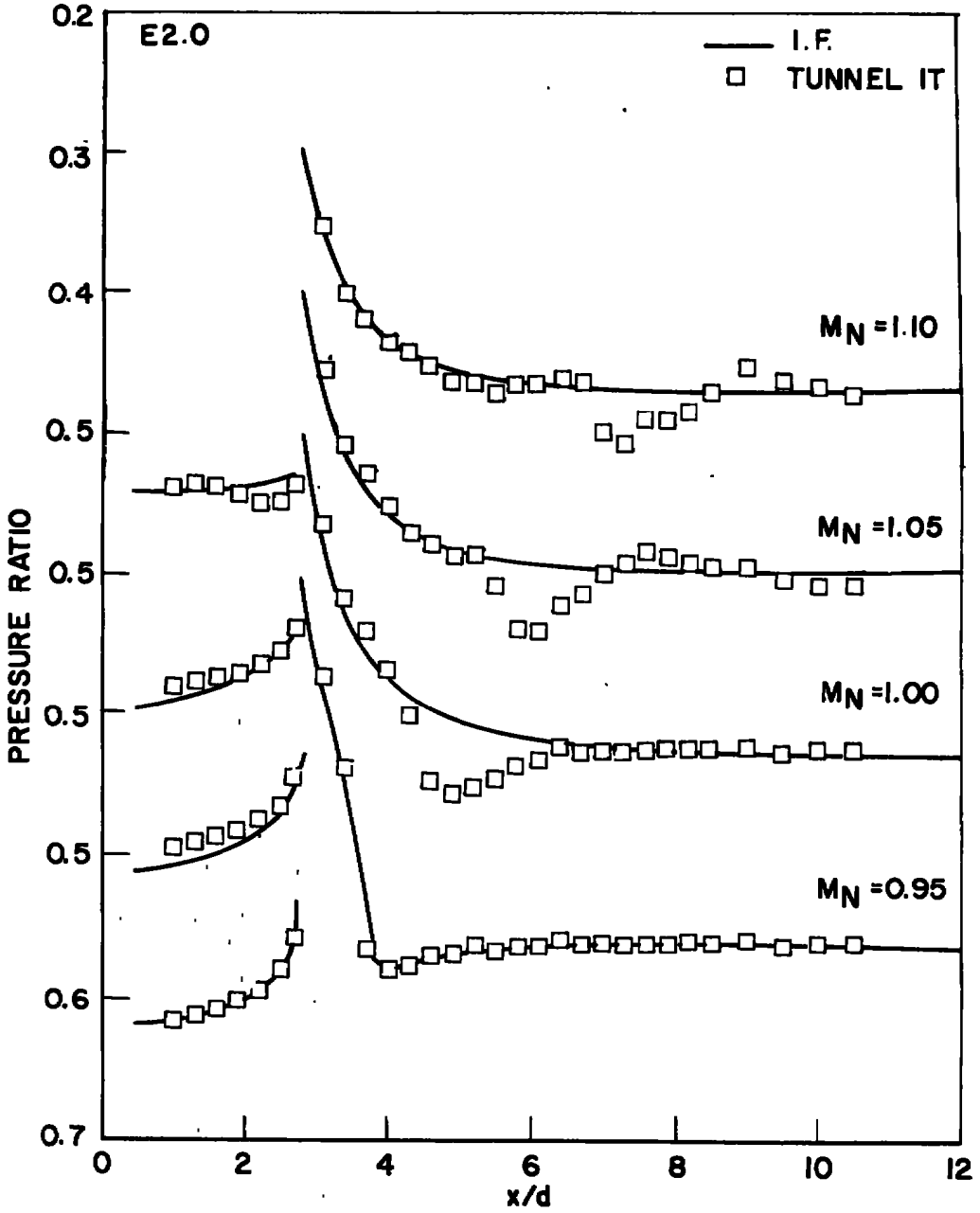

b. r = 2.0

Fig. 15 Concluded

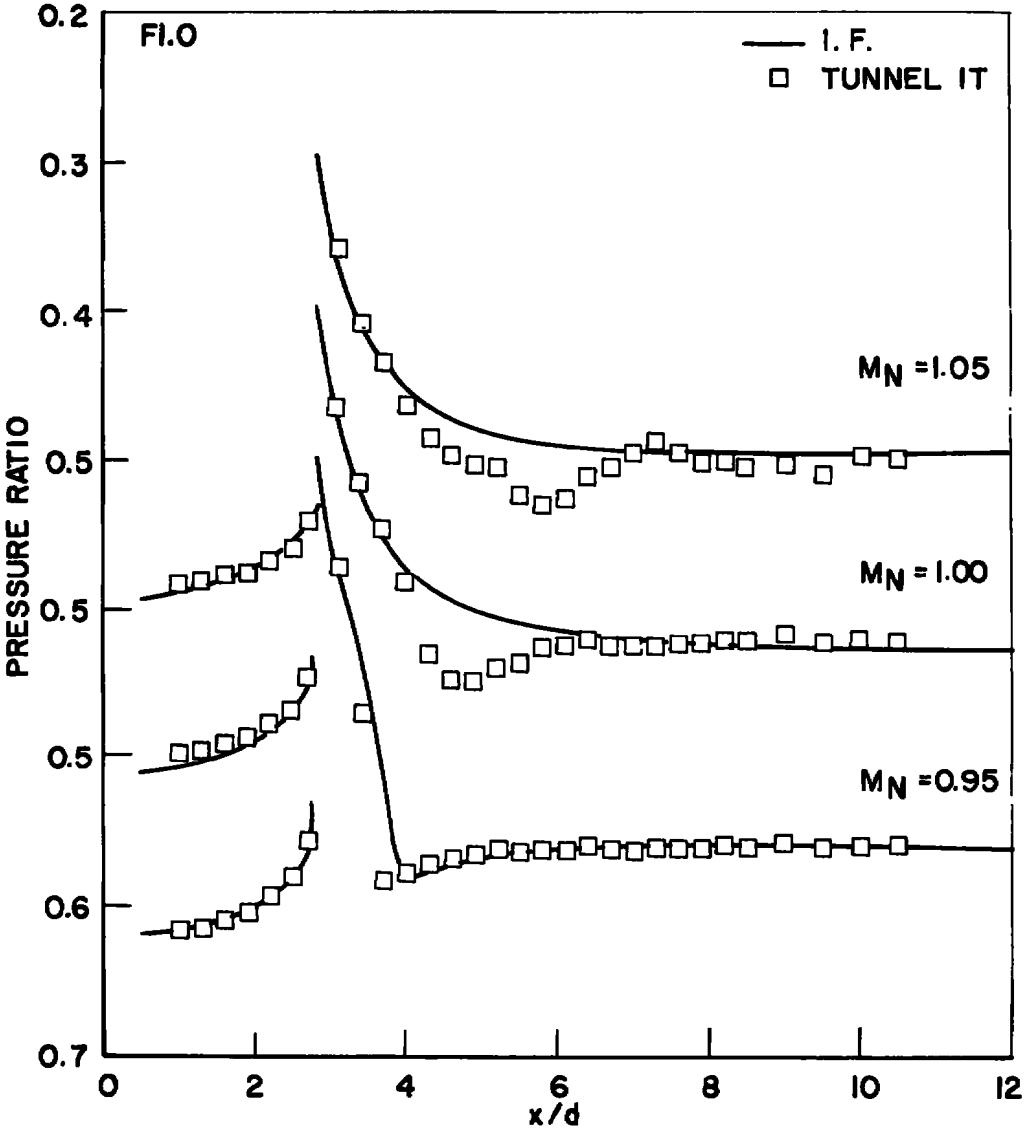

Fig. 16 Model Pressure Distributions with Wall F, θ_w = 0, τ = 1.0

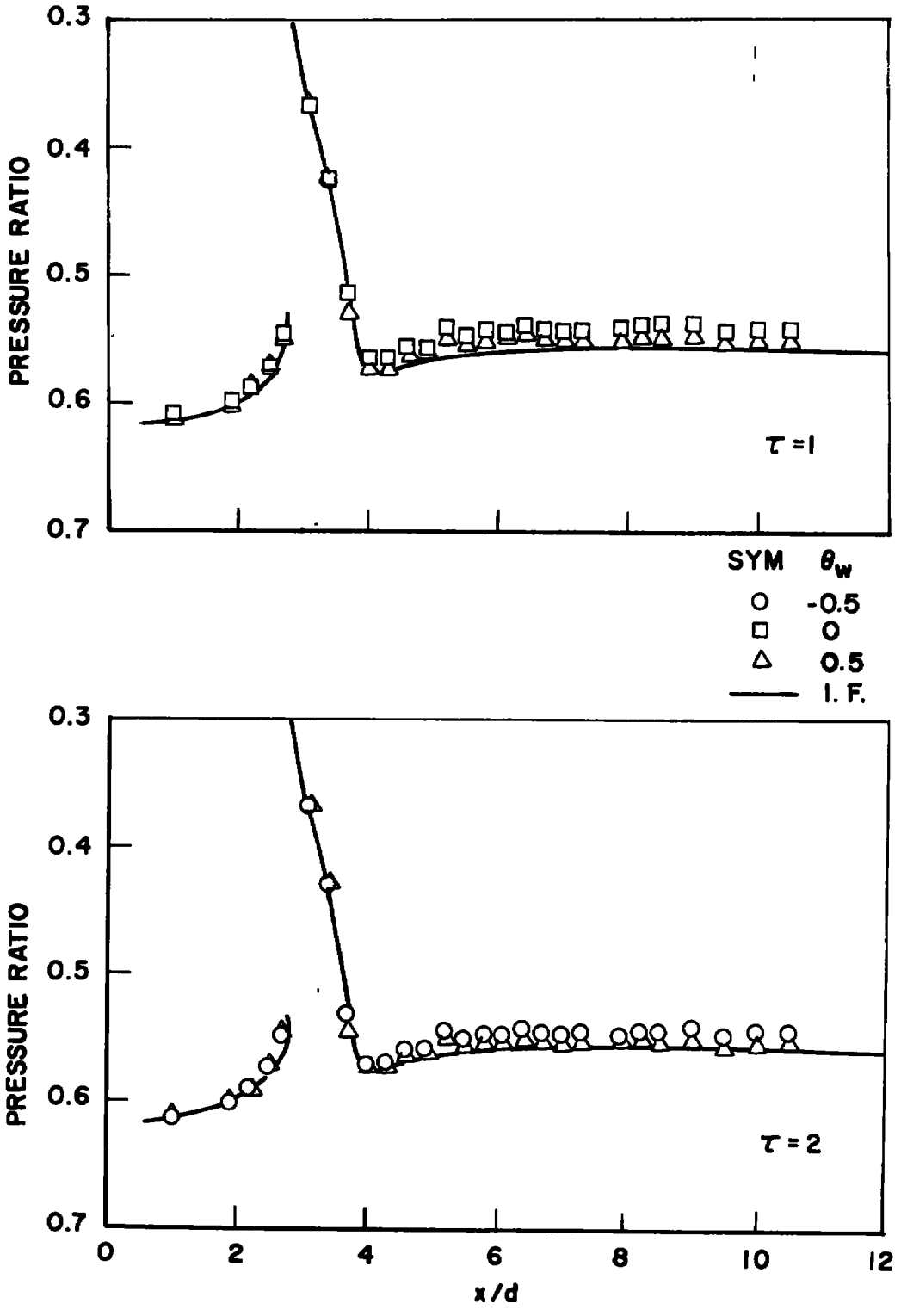

a. M_N = 0.95

Fig. 17 Influence of Wall Angle upon the Model Pressure Distributions with Wall C

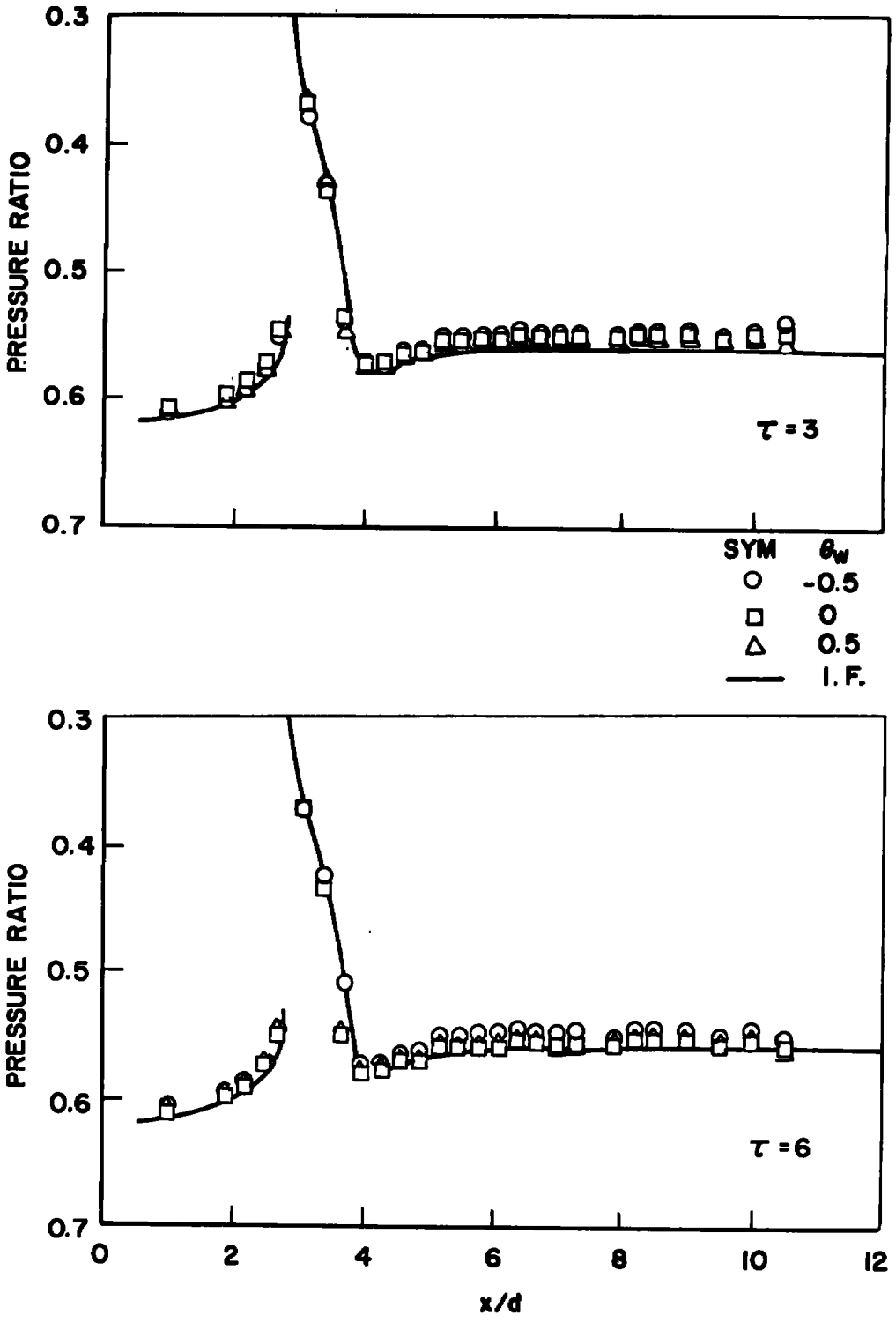

(a. Concluded

Fig. 17 Continued

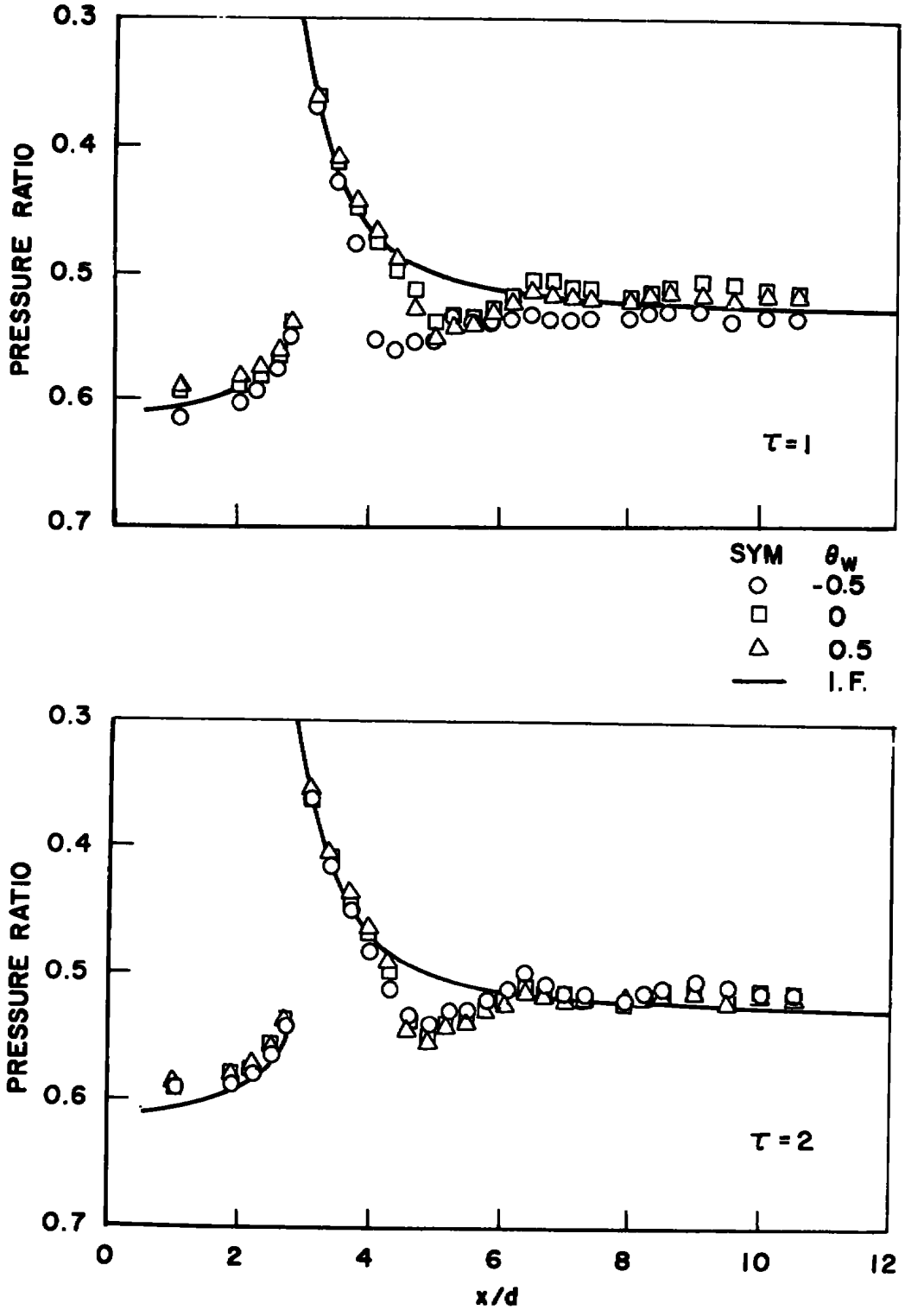

b. M_N = 1.00

Fig. 17 Continued

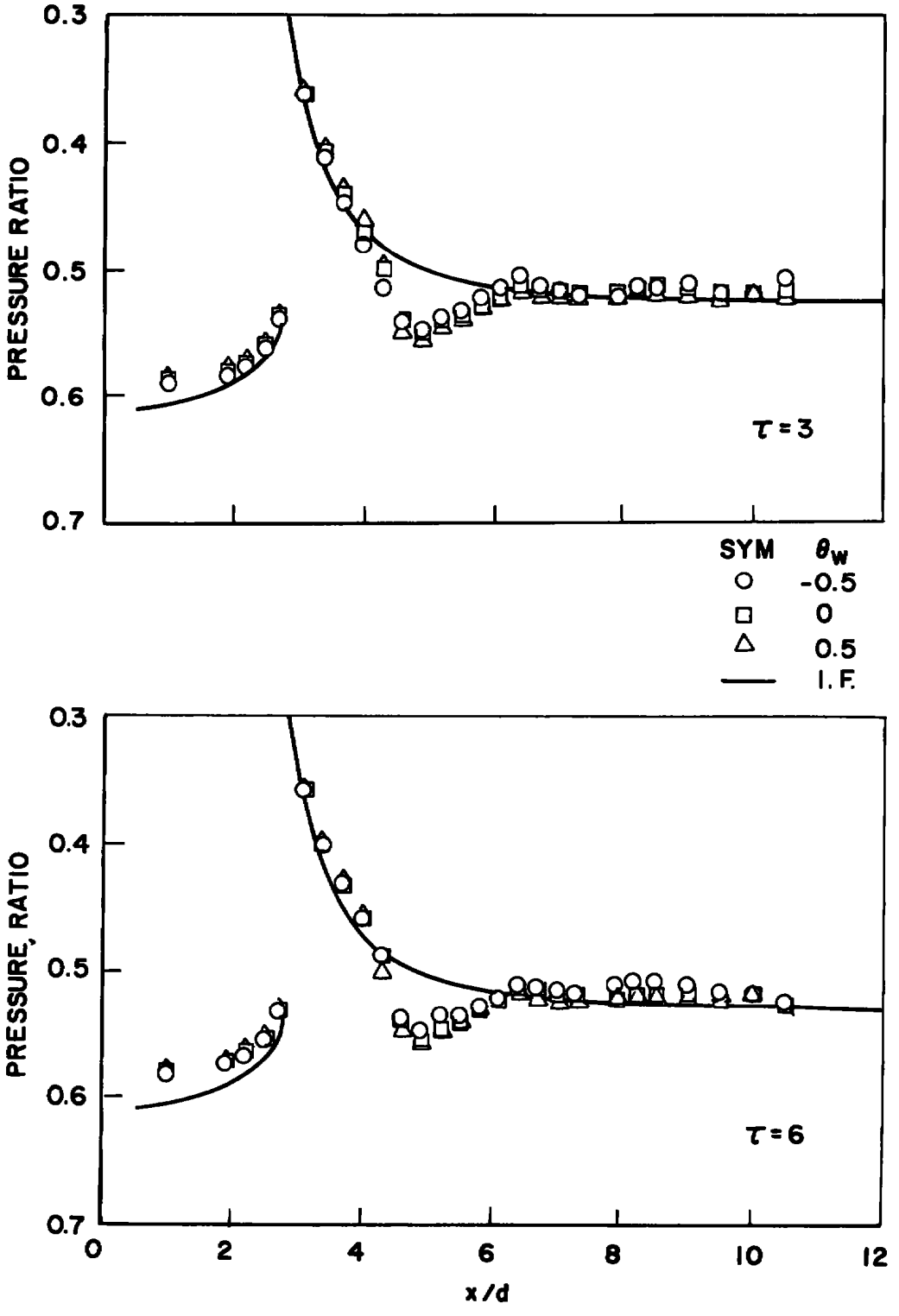

b. Concluded
Fig. 17 Continued

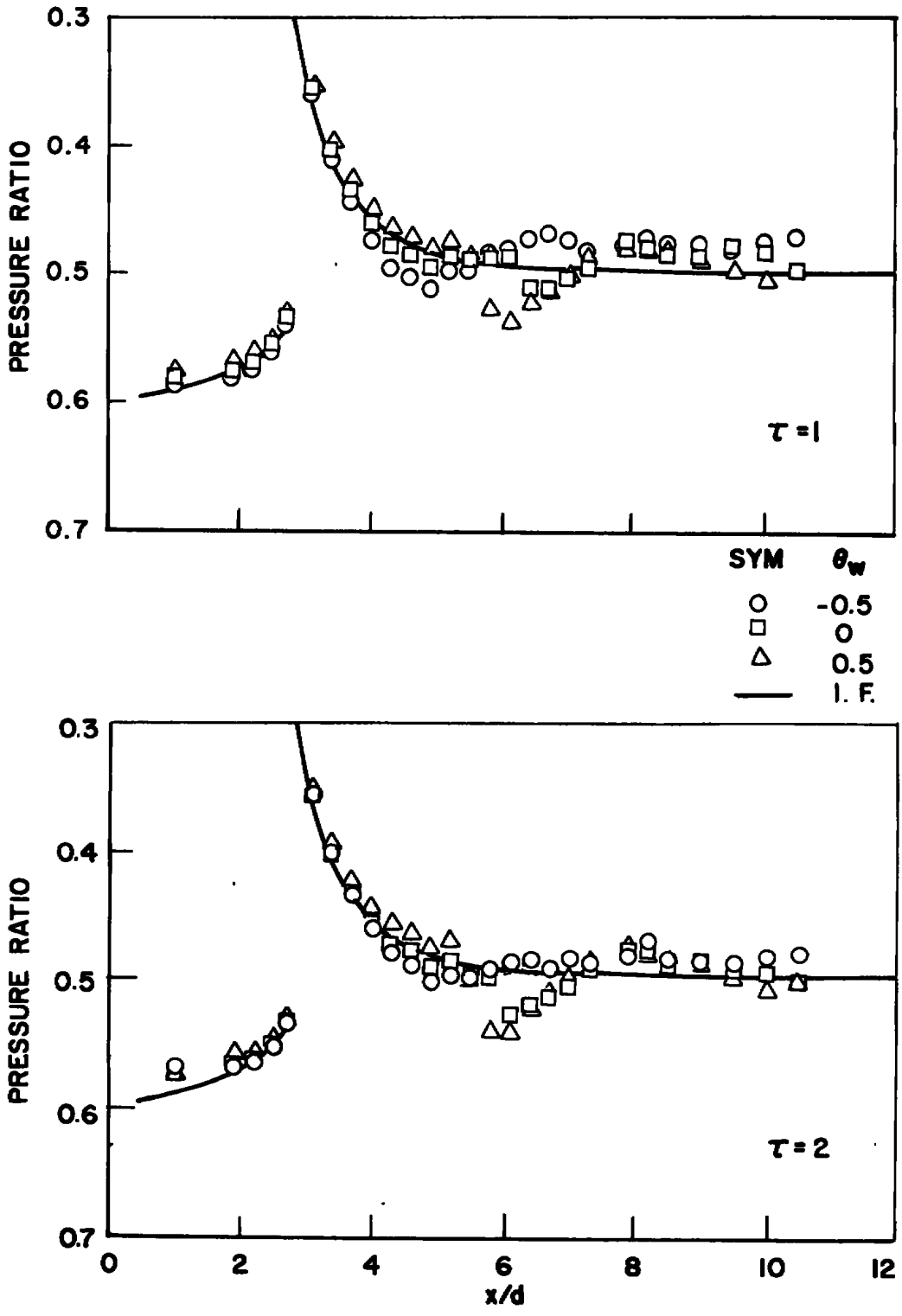

c. M_N = 1.05

Fig. 17 Continued

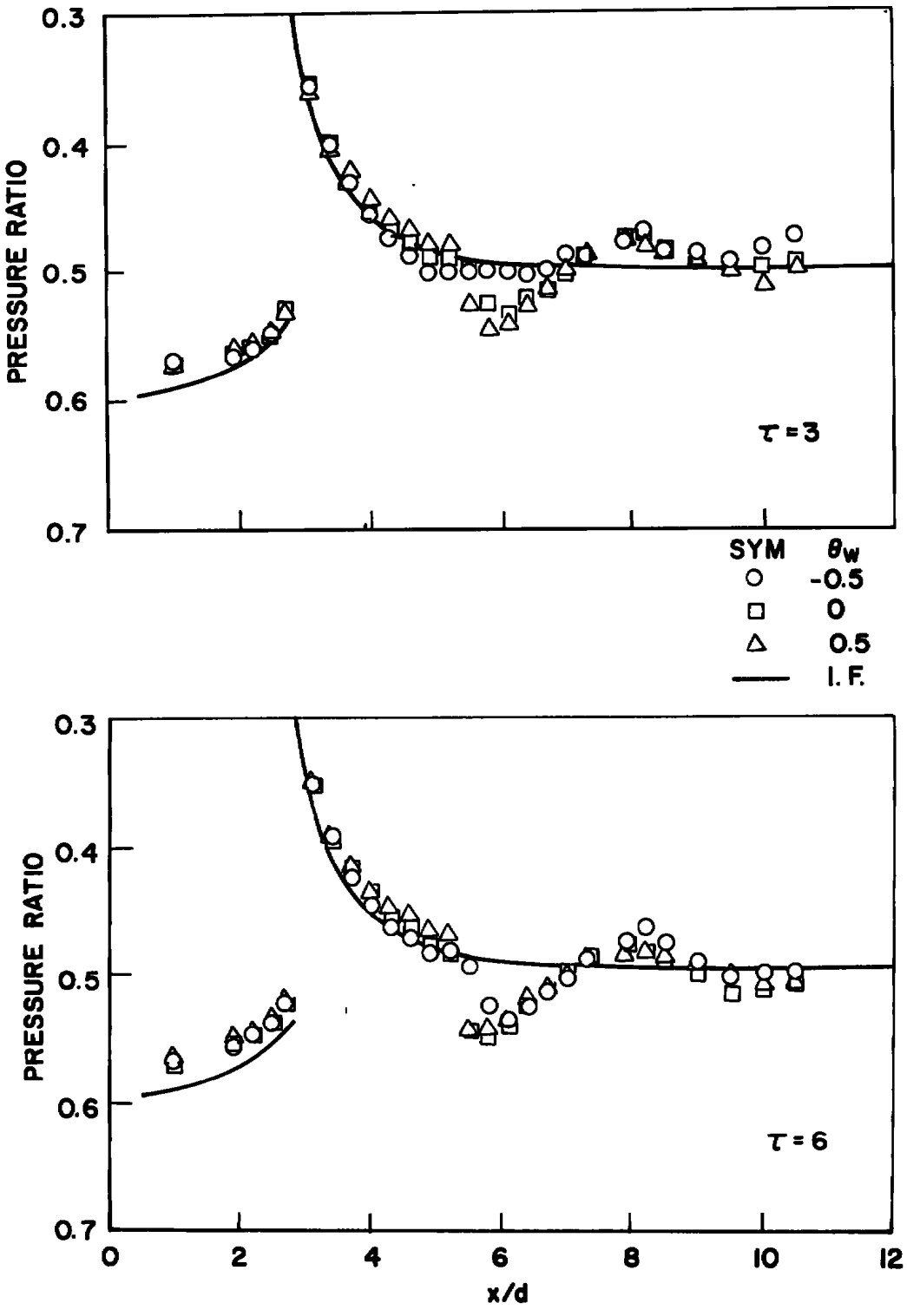

c. Concluded

Fig. 17 Continued

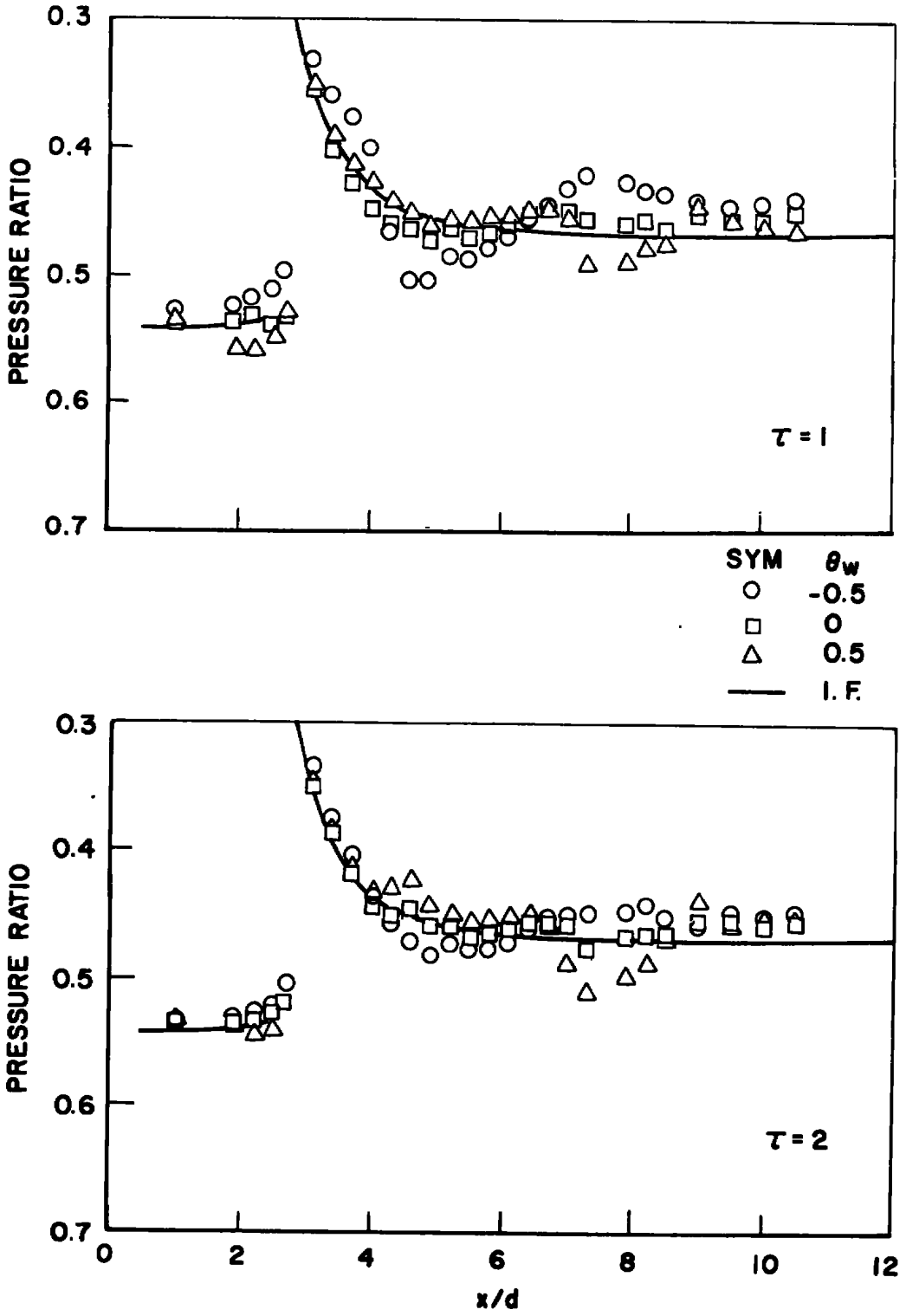

d. M_N = 1.10

Fig. 17 Continued

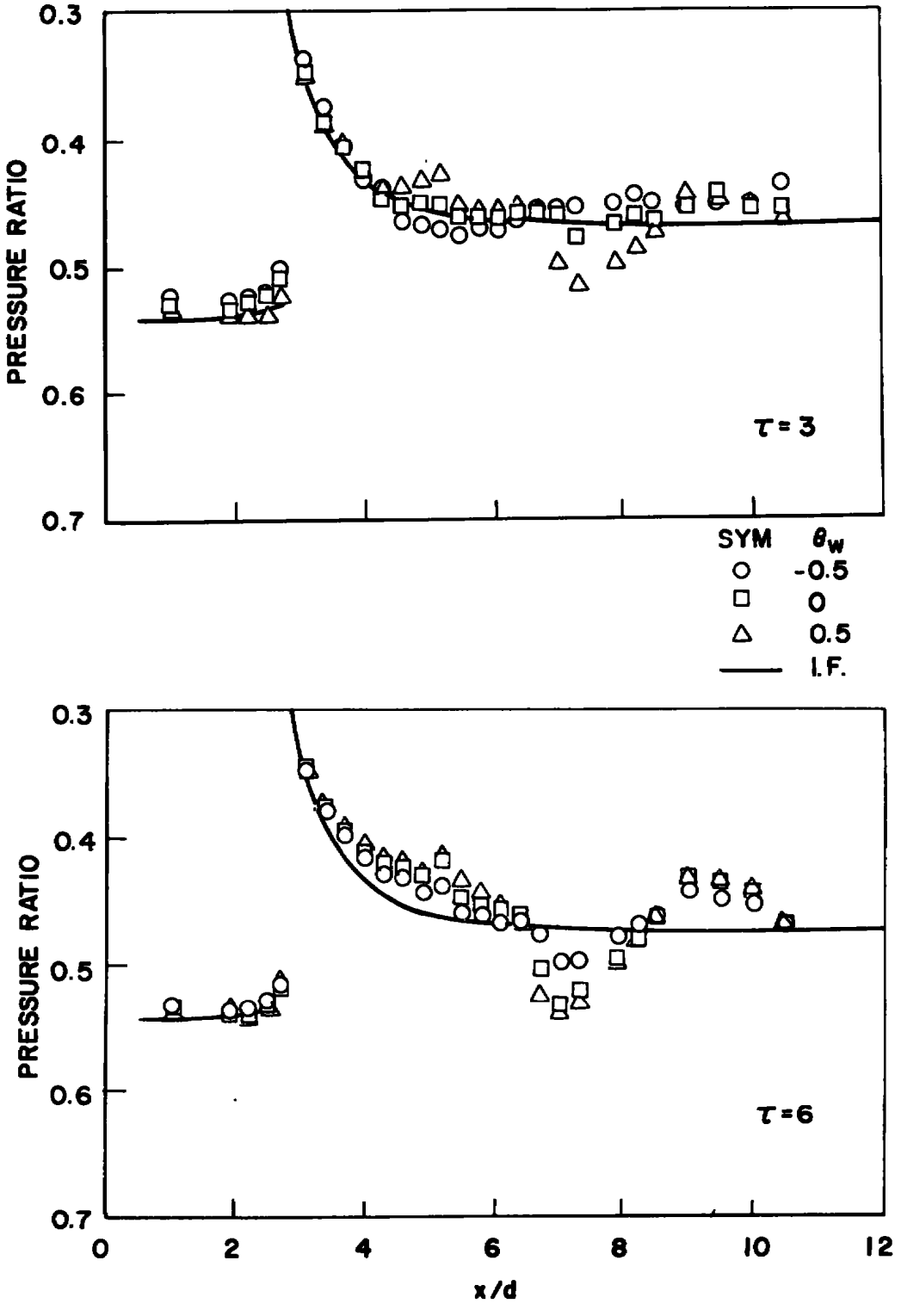

d. Concluded

Fig. 17 Continued

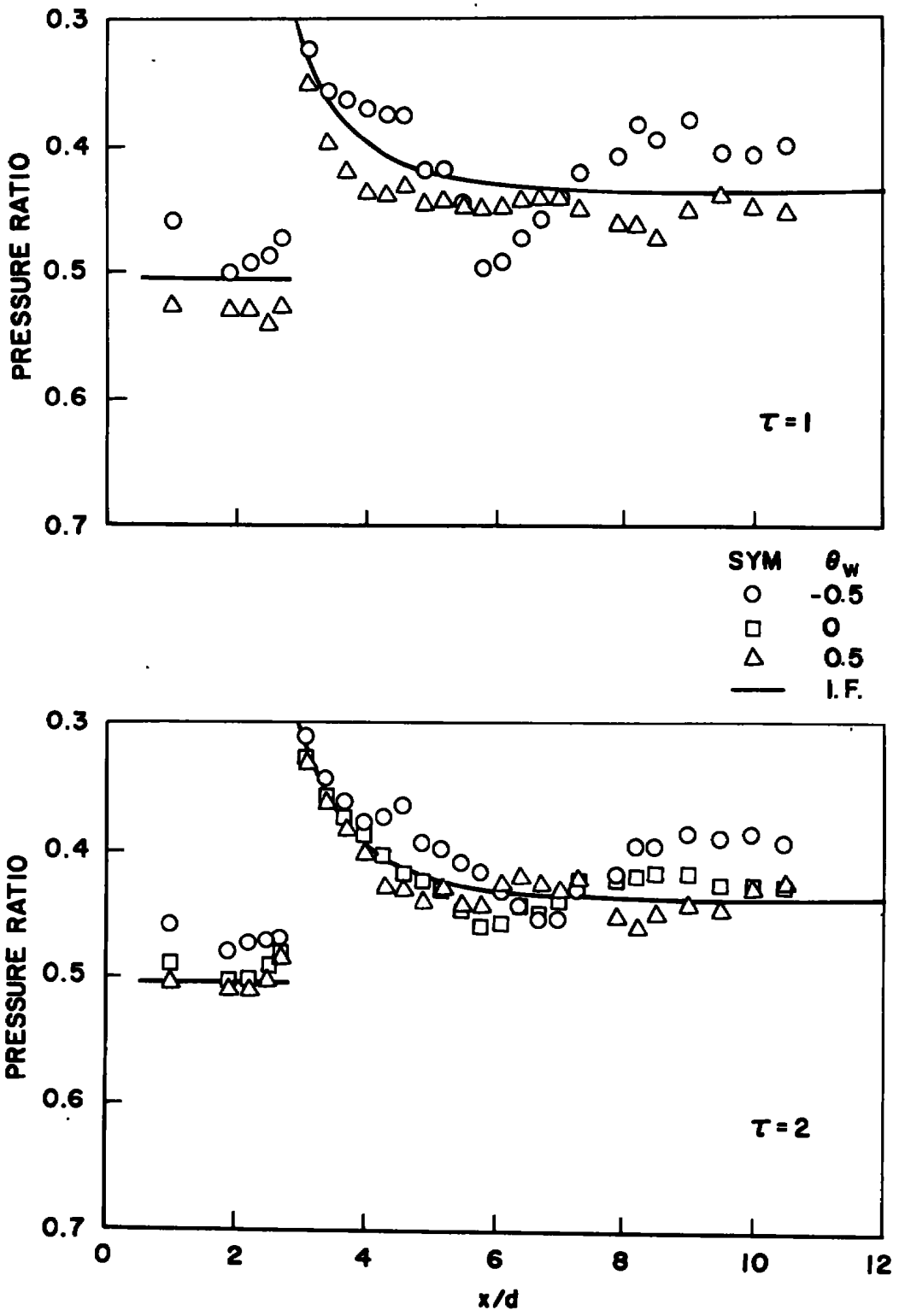

e. $M_N = 1.15$

Fig. 17 Continued

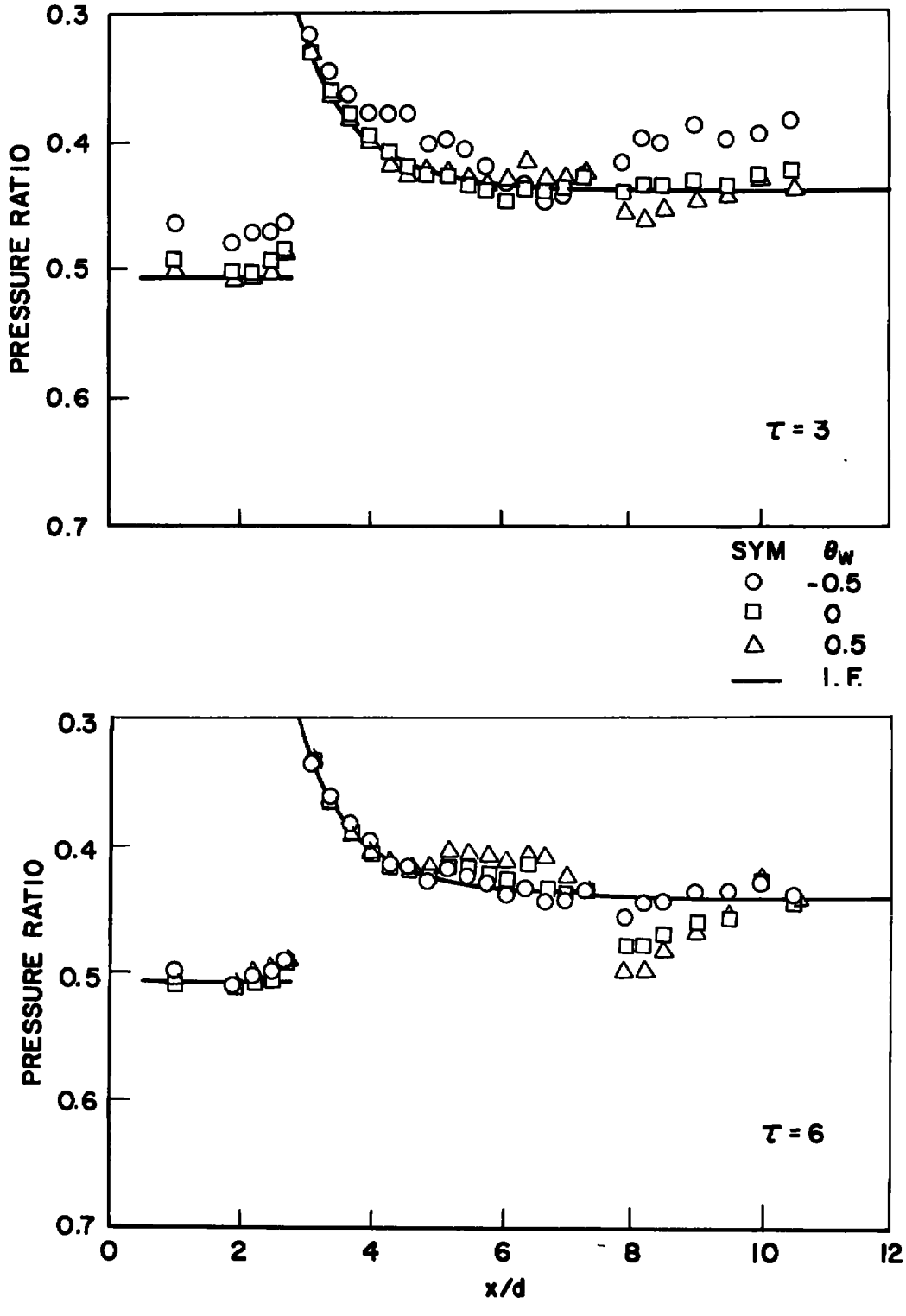

e. Concluded

Fig. 17 Continued

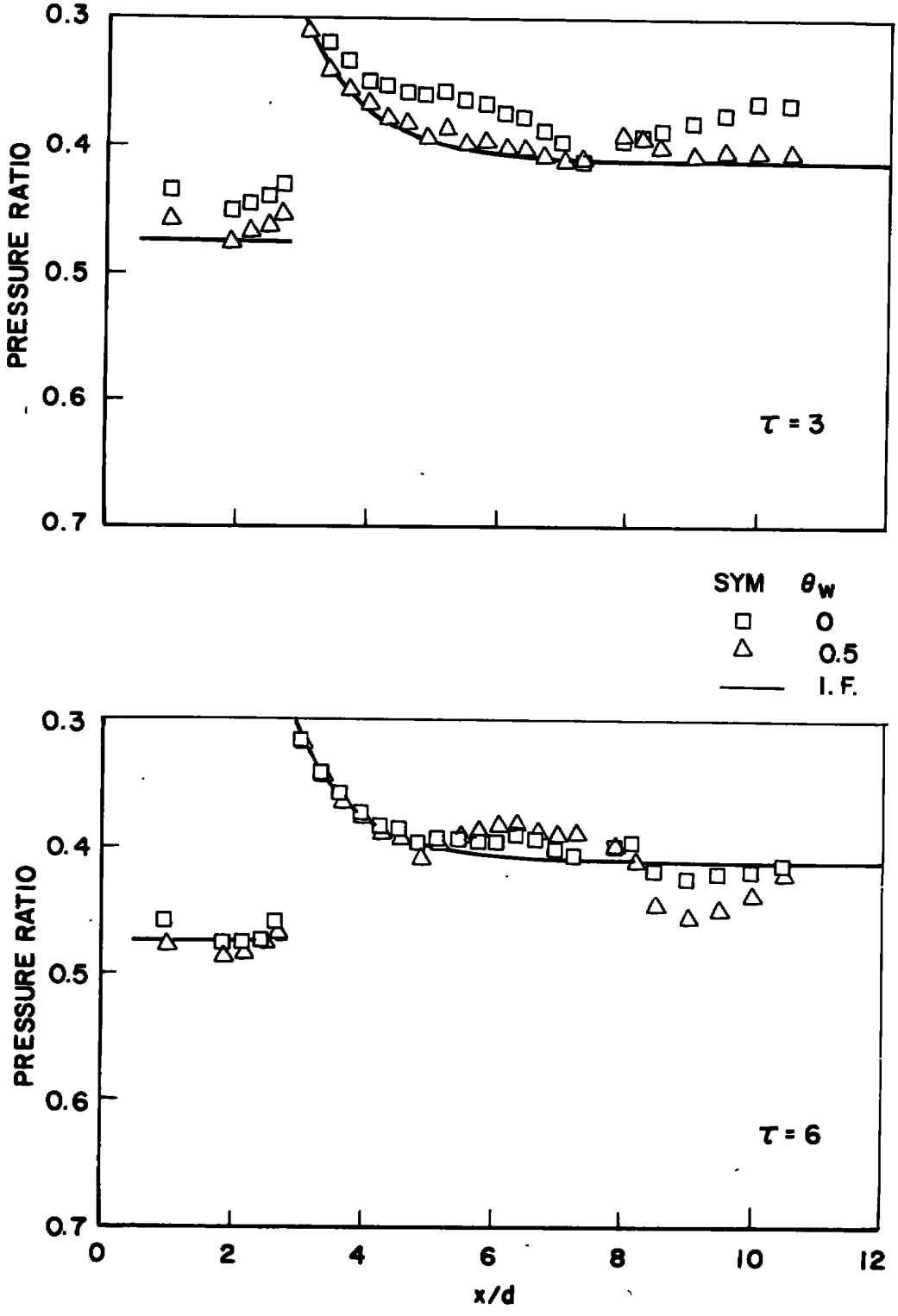

f. M_N = 1.20

Fig. 17 Concluded

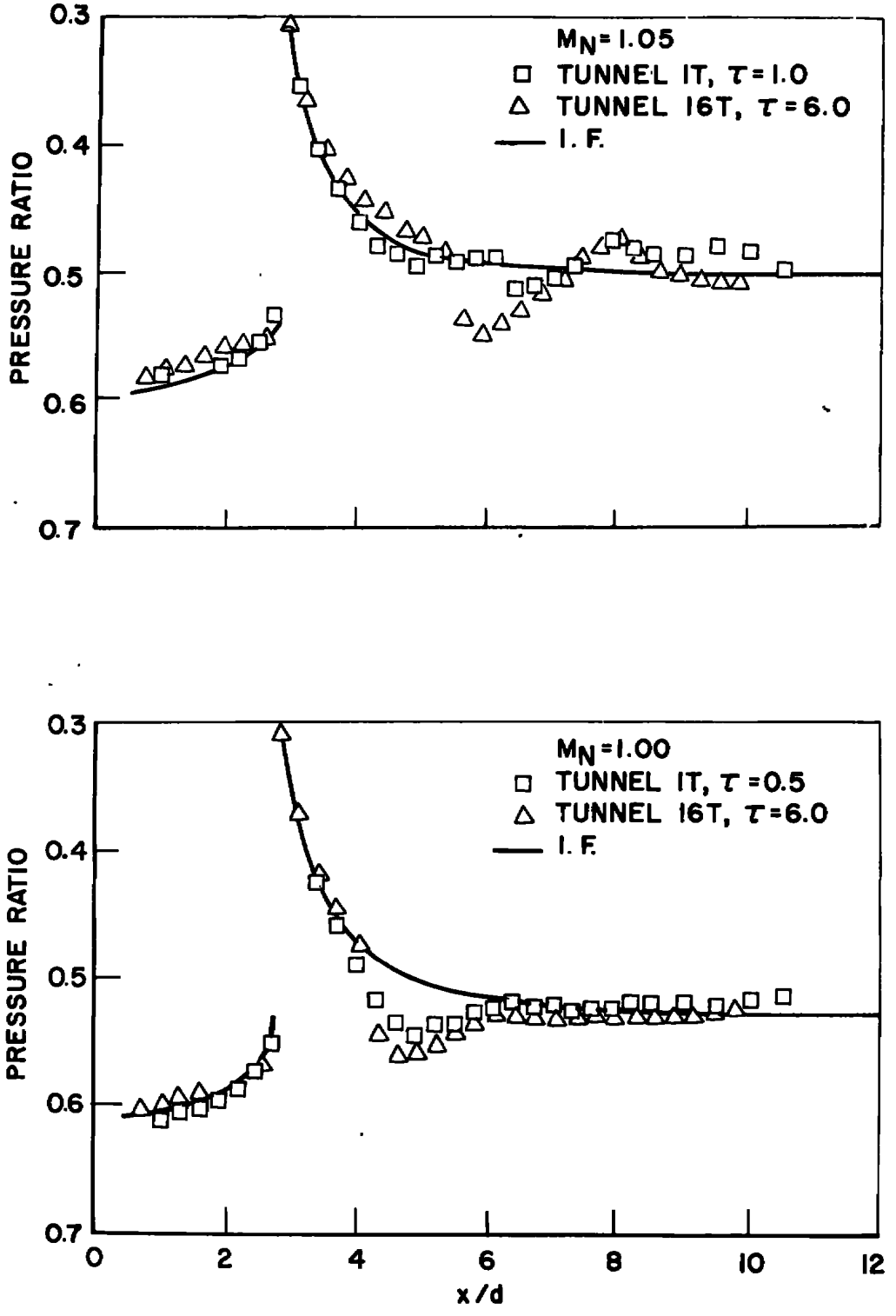

a. M_N = 1.00 and 1.05

Fig. 18 Comparison of the Model Pressure Distributions with Fixed and Variable Perforated Walls, θ_w = 0

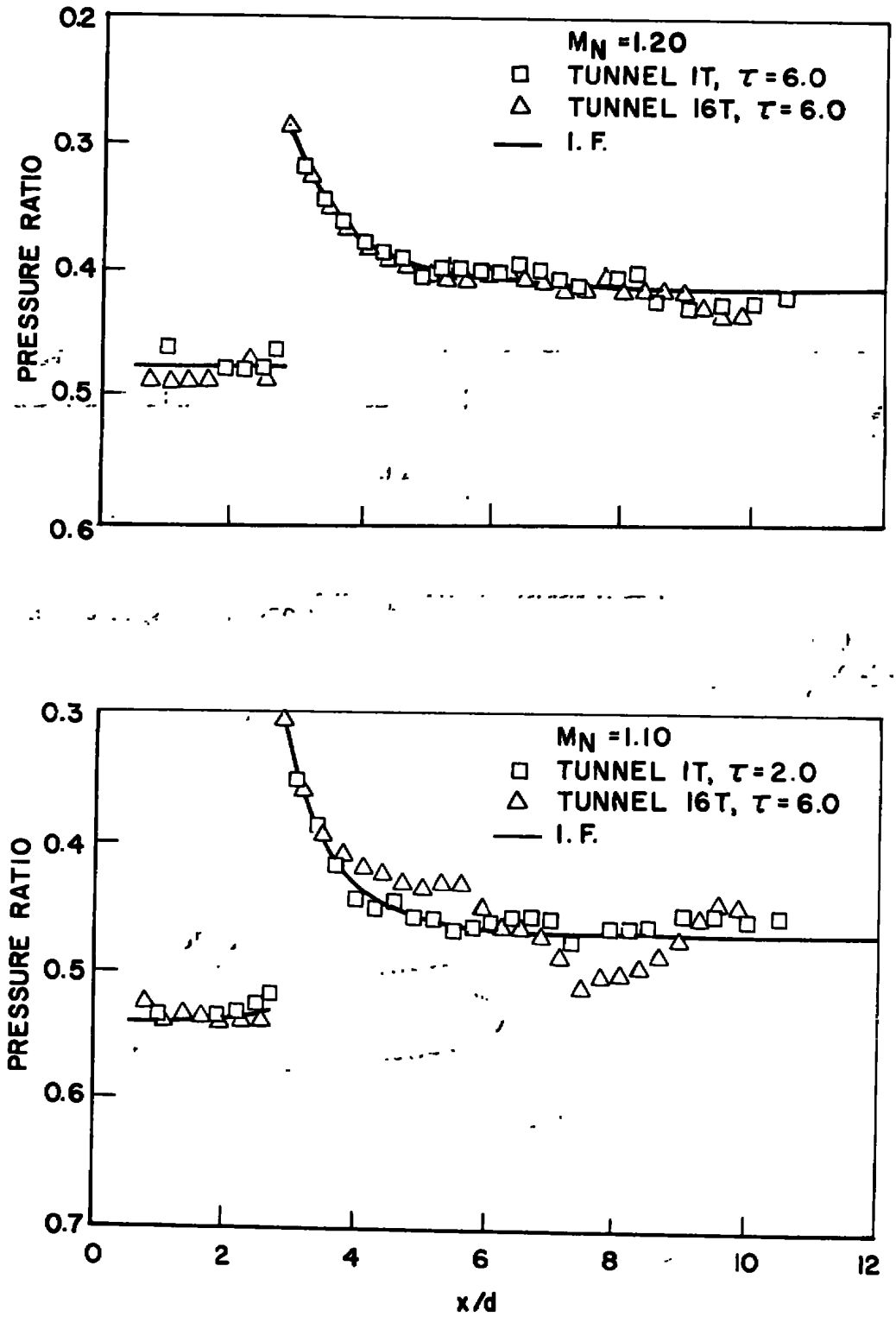

b. M_N = 1.10 and 1.20
Fig. 18 Concluded

UNCLASSIFIED

Security Classification

DOCUMENT CONTROL DATA - R & D

(Security classification of title, body of abstract and indexing annotation must be entered when the overall report is classified)

1. ORIGINATING ACTIVITY (Corporate author)	2a. REPORT SECURITY CLASSIFICATION
Arnold Engineering Development Center ARO, Inc., Operating Contractor Arnold Air Force Station, Tennessee	UNCLASSIFIED
	2b. GROUP N/A

3. REPORT TITLE

REDUCTION OF WALL INTERFERENCE EFFECTS IN THE AEDC-PWT 1-FT TRANSONIC TUNNEL WITH VARIABLE PERFORATED WALLS

4. DESCRIPTIVE NOTES (Type of report and inclusive dates)

October 8 to October 24, 1968 - Final Report

5. AUTHOR(S) (First name, middle initial, last name)

J. L. Jacocks, ARO, Inc.

6. REPORT DATE	7a. TOTAL NO. OF PAGES	7b. NO. OF REFS
May 1969	57	8

8a. CONTRACT OR GRANT NO.	9a. ORIGINATOR'S REPORT NUMBER(S)
F40600-69-C-0001 b. PROJECT NO. 06RB c. Program Element 65401F d.	AEDC-TR-69-86 9b. OTHER REPORT NO(S) (Any other numbers that may be assigned this report) N/A

10. DISTRIBUTION STATEMENT This document is subject to special export controls and each transmittal to foreign governments or foreign nationals may be made only with prior approval of Arnold Engineering Development Center (AETS), Arnold Air Force Station, Tennessee 37389.

11. SUPPLEMENTARY NOTES	12. SPONSORING MILITARY ACTIVITY
Available in DDC	Arnold Engineering Development Center (AET), Arnold Air Force Station, Tenn.37389

13. ABSTRACT

An experimental investigation was conducted in the 1-Ft Transonic Tunnel to assess the transonic wave cancellation performance of six variable porosity, test section wall designs. The wall interference effects were detected utilizing a 20-deg cone-cylinder static pressure model of 1-percent blockage. The variable wall porosity designs incorporated a sliding cutoff plate with hole geometry identical to a fixed airside plate. Upstream movement of the sliding plates for decreasing porosity provided a test section boundary which successfully eliminated wave reflection wall interference throughout most of the transonic range.

This document is subject to special export controls and each transmittal to foreign governments or foreign nationals may be made only with prior approval of Arnold Engineering Development Center (AETS), Arnold Air Force Station, Tennessee 37389.

DD FORM 1 NOV 65 1473

UNCLASSIFIED

Security Classification

14. KEY WORDS	LINK A ROLE	LINK A WT	LINK B ROLE	LINK B WT	LINK C ROLE	LINK C WT
transonic wind tunnels						
conical bodies						
pressure distribution						
walls						
porosity						
performance						
wave interference						

1. Transonic wind tunnels -- Interfer -- PCWT
2 " " " -- Perform
3 Porous wall wind tunnels -- 4
-- PCWT
5 " " " "

173

AFSC
Arnold AFS Tenn